OF HIS BONES ARE CRINOID MADE: TAPHONOMY AND DEADFALL ECOLOGY OF MARINE REPTILES FROM A PELAGIC SETTING (MIDDLE-UPPER JURASSIC OF NORTHEASTERN ITALY)

GIOVANNI SERAFINI[1], SILVIA DANISE[2], ERIN E. MAXWELL[3], LUCA MARTIRE[4], JACOPO AMALFITANO[5], MIRIAM COBIANCHI[6], URSULA THUN HOHENSTEIN[7, 8] & LUCA GIUSBERTI[5]

[1]Dipartimento di Scienze Chimiche e Geologiche, Università di Modena e Reggio Emilia, Via Campi 103, 41125, Modena, Italy.
[2]Dipartimento di Scienze della Terra, Università degli Studi di Firenze, Via La Pira, 4, 50121, Firenze, Italy
[3]Staatliches Museum für Naturkunde Stuttgart, Rosenstein 1, 70191 Stuttgart, Germany.
[4]Dipartimento di Scienze della Terra, Università degli Studi di Torino, Via Valperga Caluso, 35, 10125 Torino, Italy
[5]Dipartimento di Geoscienze, Università degli Studi di Padova, Via Gradenigo 6, I-35131, Padova, Italy
[6]Dipartimento di Scienze delle Terra e dell'Ambiente, Università di Pavia, Via Ferrata 1, I-27100, Pavia, Italy.
[7]Dipartimento di Studi Umanistici, Università degli Studi di Ferrara, Corso Ercole I d'Este, 44121, Ferrara, Italy
[8]Museo di Paleontologia e Preistoria "Piero Leonardi", Sistema Museale di Ateneo, Università degli Studi di Ferrara, Italy.

Abstract. Modern cetaceans are considered the best anatomical and ecological analogue for many Mesozoic secondary aquatic reptiles. Such similarities extend also after the death of these phylogenetically distant amniotes, when the sinking and decomposition of large carcasses in marine environments (deadfalls) follow common biostratinomic processes. Most taphonomic studies on Mesozoic deadfalls have been limited to shallow-water settings, often neglecting deeper waters. Here we provide a detailed taphonomic survey of ichthyosaurs, pliosaurs and metriorhynchoids from the pelagic Middle-Upper Jurassic Rosso Ammonitico Veronese (RAV) of northeastern Italy. Our taphonomic revision of the RAV tetrapod record highlights a common poor state of preservation of the bones, often associated with abundant macrofossils, consistent with a prolonged exposure of carcasses on a well-oxygenated seafloor. For the first time we confirm the role of nautiloids as active mobile scavengers by means of tens of beak elements found closely associated with, or even piercing, the bones. Hexanchiform shark teeth are also found associated with the carcasses, supporting a distinctive deep-water mobile scavenging community. Echinoids, sponges and other bioeroders are identified as representative of the enrichment-opportunist stage, and a high concentration of belemnites is believed to be indicative of mass-spawning deaths in the surroundings of the carcasses. Abundant crinoids are recognized as part of the reef stage by colonization of the eroded bones. While some of our data deviate from previous Mesozoic reptile-falls from shallow-waters, they are consistent with findings at Recent whale-falls in bathyal zones, and overall represent a precious window into the complex ecology of Jurassic open seas.

INTRODUCTION

In modern oceans, sunken carcasses of large vertebrates play an essential role in the flux of carbon, nitrogen, sulfur and phosphorus in deep-water

(i.e., below the shelfbreak) settings, providing different classes of nutrients during different stages of decay (Smith et al. 2015). Thanks to such transfer of energy, vertebrate deadfalls generate peculiar though ephemeral ecosystems around them (Allison et al. 1991; Smith & Baco 2003; Higgs et al. 2014; Smith et al. 2015), with highly specialized organisms attract-

ed by the massive availability of nutrients released during the carcass break down. These successions are diverse in taxonomic composition, ranging from bacteria to vertebrates, and represent true islands of species and individual abundance in otherwise poorly biodiverse zones (Glover et al. 2005; Treude et al. 2009; Smith et al. 2015). Any large vertebrate-fall (also fish-falls, e.g., whale sharks or manta rays; Higgs et al. 2014) could provide enough nutrients for the development of specialized ecological communities, but only in the case of cetaceans (particularly mysticetes) an exceeding amount of fats, proteins, sugars and minerals can sustain a deadfall community for decades (Smith & Baco 2003; Goffredi et al. 2008; Treude et al. 2009). Within the specific case study of whale-falls, Smith & Baco (2003) formalized four stages of ecological community succession during carcass exploitation in deep-water settings:

1) Mobile scavenger stage: the removal of soft tissue on the carcass when floating in the water column or at the seafloor by the activity of nektonic necrophages such as sharks, fishes, myxines, isopods and cephalopods (Martini 1998; Clua et al. 2013; Smith et al. 2015).

2) Enrichment-opportunist stage: colonization of the skeletonized carcass and surrounding enriched sediment by invertebrates and microbial mats. This phase often features ampharetid and hesionid polychaetes, decapod crustaceans, ophiuroids, bivalves, *Beggiatoa* microbial mats, and, most distinctively, osteophagous siboglinid polychaetes of the genus *Osedax* (Glover et al. 2005; Smith et al. 2015; Georgieva et al. 2023).

3) Sulfophilic stage: microbial metabolization of bone lipids by sulfur-reducing bacteria (e.g., *Desulfobacter*) and competing/coexisting methanogenic archaea (Goffredi et al. 2008; Goffredi & Orphan 2010). This initial microbial wave is usually followed by the activity of hydrogen sulfide-oxidizing chemosynthetic bacteria, either free living or as symbionts of metazoans such as lucinid, thyasirid and vesicomyid bivalves (Treude et al. 2009; Goffredi & Orphan 2010; Smith et al. 2015).

4) Reef stage: once the skeleton has exhausted all its organic nutrients, it is used as a hard substrate for the growth of encrusting filter-feeding organisms (e.g., ostreids, serpulids; Danise & Dominici 2014; Smith et al. 2015).

All four stages were indirectly observed in the fossil record of whales, framing these special-ized ecological successions in deep time (see Danise et al. 2012; Danise & Dominici 2014 and references therein). Besides their pure biomass, cetacean deadfalls ensure rich and prolonged ecological successions due also to the high lipid content of their bones; lipid availability is pivotal for the development of communities that exploit skeletal remains (Smith & Baco 2003; Danise et al. 2014) and highly cancellous bone serves as a storage for fats essential to the buoyancy and high metabolism of fully pelagic secondarily aquatic amniotes (Houssaye et al. 2014, 2018; De Buffrénil et al. 2021). Since the very beginning of whale-fall studies, it was speculated that Mesozoic marine reptiles could have played a similar role to that of cetaceans after death, possibly triggering the evolution of whale-fall specialist precursors or of their analogues as far back as the Jurassic (Martill et al. 1991; Hogler 1994). Ichthyosaurs, metriorhynchids, some plesiosaurs and mosasaurs share anatomical similarities with modern cetaceans, such as an anteriorly shifted center of mass, reduced limb girdles (with the exception of plesiosaurs), hydropedal limbs and an osteoporotic-like bone microstructure that could host high amounts of lipids (Houssaye et al. 2018; Gutarra & Rahman 2021). These anatomical analogies imply a similar taphonomic pathway and the possibility of producing similar deadfall communities. Although most of our knowledge of modern whale-fall communities comes from the deep sea (Smith & Baco 2003; Fujiwara et al. 2007; Smith 2015), most previous taphonomic studies on fossil marine reptiles from Europe were carried out on material from epicontinental Fossil-Lagerstätten, namely the Oxford Clay of the UK (e.g., Martill 1985), the Posidonia Shale of southern Germany (e.g., Martill 1993; Beardmore et al. 2012; Beardmore & Furrer 2016) and the Slottsmøya member in Spitsbergen (Delsett et al. 2016). The most detailed studies to date focusing specifically on Mesozoic deadfall communities (Danise et al. 2014; Dick 2015; Delsett et al. 2016; Maxwell et al. 2022) come from the same shallow deposits. Outside Europe, taphonomic surveys on marine vertebrates also focused mostly on shallow-water settings (e.g., Schmeisser McKean & Gillette 2015), with very few exceptions from continental slopes (Kaim et al. 2008; Stinnesbeck et al. 2014; Sato & Jenkins 2020). As a consequence, very little is known on preservation patterns and deadfall ecology from epipelagic to abyssopelagic settings during

the Mesozoic. Pelagic deposits are usually not suited for vertebrate preservation, since slow sedimentation rates preclude fast burial of the remains (Allison et al. 1991; Serafini et al. 2020); these units can, however, yield precious taphonomic and paleoecological insights on the role of large carcasses in deep-water trophic networks, as slow sedimentation rates may ensure enough exposure time of the remains for the development of deadfall ecological successions.

Here we present a detailed taphonomic revision of the tetrapod record from the Rosso Ammonitico Veronese (henceforth shortened to RAV) of northeastern Italy, a pelagic deposit opened to oceanic circulation on the western side of the Tethys Ocean and ranging from the Middle to Upper Jurassic (Bajocian-Tithonian). Despite its rather poor record, RAV marine reptiles have been the subject of several taxonomic and evolutionary studies in the past (e.g., Cau & Fanti 2011, 2014, 2016; Cau 2019) but only recently has attention been brought to the taphonomy of individual specimens (Serafini et al. 2020, 2022, 2023a,b). First, our analysis subdivides the record into specific taphofacies based on a characterization of their skeletal and dental tissue preservation. Then, ichthyosaurs, thalattosuchians and plesiosauroids are surveyed for their associated fossil fauna to reconstruct deep-water deadfall stages.

GEOLOGICAL SETTING

The marine tetrapod record surveyed for this study comes from three separate areas of the Southern Alps of northeastern Italy (Fig. 1A, B): the Asiago Plateau (Vicenza Province), from where most of the specimens derive, the Belluno area, and the S. Ambrogio di Valpolicella area (Verona Province). Starting from the Early Jurassic (Hettangian), all the aforementioned areas were part of the Trento Platform (Fig. 1A), a carbonate platform bordered by the deeper Lombardian and Belluno basins (e.g., Winterer & Bosellini 1981; Fig. 1A). In the Middle Jurassic, this structural high, a horst block of the southern continental margin of the Tethys, definitively drowned, becoming an articulated current-swept plateau with reduced pelagic sedimentation, leading to the deposition of the Rosso Ammonitico Veronese (RAV: Winterer & Bosellini 1981; Massari & Westphal 2011). The RAV extends from the upper Bajocian to the upper Tithonian (Winterer

& Bosellini 1981; Martire 1996; Martire et al. 2006; Fig. 1C). It is a lithologically very distinctive pelagic limestone, with a whitish- to dark-red color, frequent nodular texture and common ammonite internal molds (e.g., Clari et al. 1984; Pavia et al. 1987; Sarti 1993; Martire 1996). This limestone has been actively quarried in northern Italy since Roman times (Barbieri & Ginevra 1995). Martire et al. (2006) formalized three lithostratigraphic subdivisions of the unit: the Rosso Ammonitico Inferiore (RAI; upper Bajocian–upper Callovian), characterized by massive and calcareous lithology and pseudonodular facies, the Rosso Ammonitico Medio (RAM; middle Callovian–middle Oxfordian), characterized by thin-bedded, planar-parallel- to flaser-bedded limestones locally associated with nodules and layers of red chert, and the Rosso Ammonitico Superiore (RAS; middle Oxfordian–upper Tithonian), which consists of pink-red, nodular, ammonite-rich limestones (Martire 1996; Martire et al. 2006). RAI commonly contains microbialites, sporadically occurring also in the lower part of the RAS (e.g., Martire et al. 2006; Massari & Westphal 2011). Macrofaunal elements of RAV mostly include ammonites (usually preserved as internal molds), belemnites, bivalves (mostly thin-shelled forms), gastropods, brachiopods, aptychi and rhyncholites, rare nautiloid internal molds, small solitary thecocyathid corals, crinoidal elements and scattered echinoids (e.g., Martire 1996; Massari & Westphal 2011). The RAS grades into the Maiolica (upper Tithonian–lower Aptian), a formation represented by thin-bedded, whitish, cherty, pelagic limestones originated, with noteworthy facies homogeneity, from the widespread deposition of calcareous nannofossil and calpionellid oozes (Martire et al. 2006). The Cretaceous pelagic sedimentation ends in the area with the deposition of the alternating limestone/marlstone whitish and grayish sediments of Scaglia Variegata Alpina, and the pink and reddish limestones and marly limestones of Scaglia Rossa.

RAV PALEOENVIRONMENT AND DEPTH SPECULATIONS

The open marine RAV succession has been regarded as mostly deposited in an aerobic setting (holoaerobic sediment), as testified by the oxidized (ferric) state of iron and by the great density of burrows and lack of trace fossils indicative of low
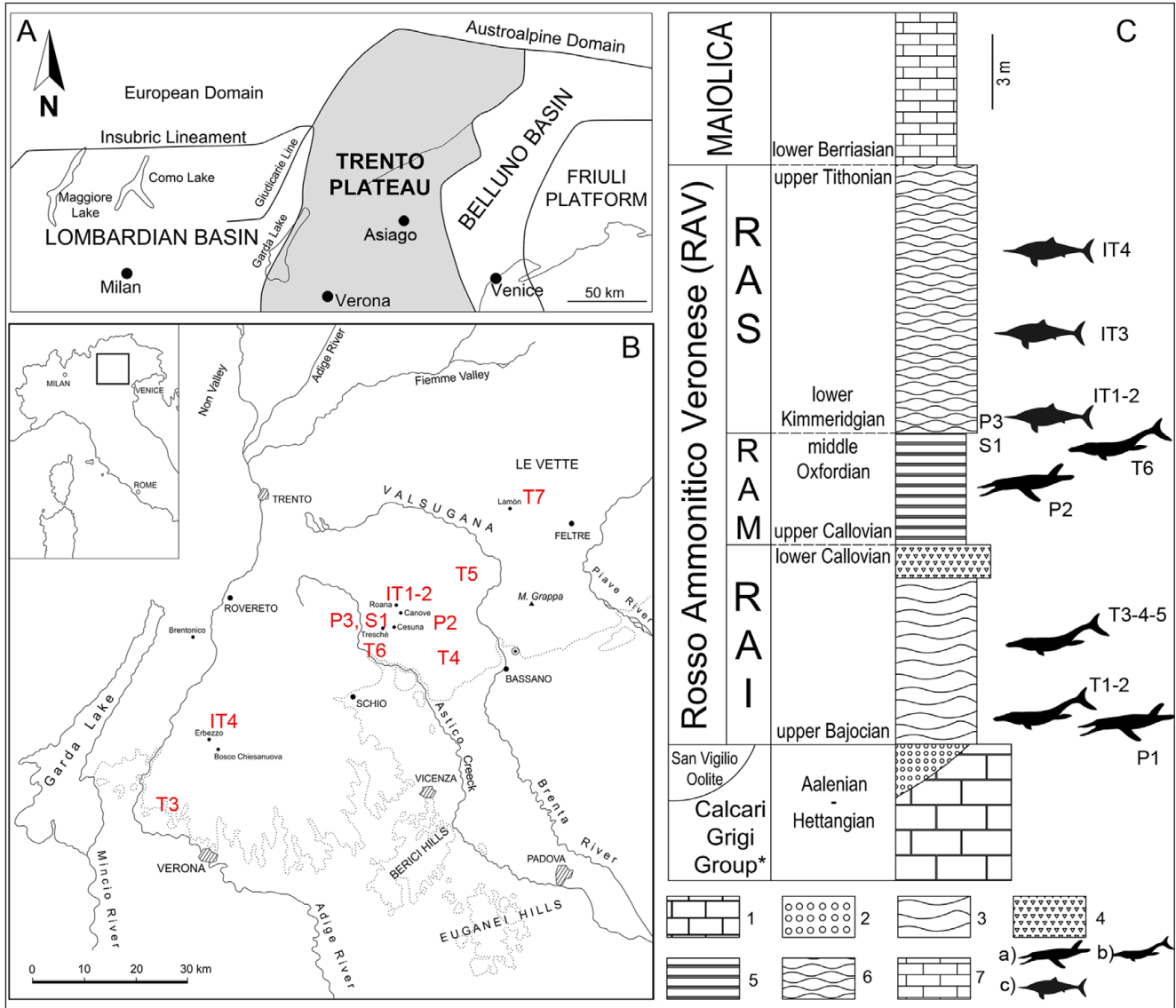
Fig. 1 - Geographic and stratigraphic context. A) Jurassic paleogeographic domains of northeastern Italy projected over the present-day geography (modified after Bosellini et al. 1981). B) Location map of the study area with indication of the localities that yielded marine reptile remains from the Rosso Ammonitico Veronese (RAV) (see Table 1 for numeration); specimens for which the precise source location is unknown are not reported in the map. C) Stratigraphy of the RAV in the Trento Plateau (Verona area and Asiago Plateau) with inferred stratigraphic position of each tetrapod specimen so far recovered in the RAV and herein listed. Silhouettes: a) Plesiosauroidea (modified after pliosauroidea outlines by Eotyrannu5, CC BY-SA 4.0); b) Metriorhynchoidea (modified after Young et al. 2012 by Dimitry Bogdanov, CC-BY 2.5); c) Ichthyosauria (modified after Sissons et al. 2015). Lithostratigraphic and lithologic legend: 1) Hettangian-Domerian shallow-water limestones of the Calcari Grigi Group (Asiago Plateau); 2) Toarcian-Aalenian oolithic limestones of the San Vigilio Oolite (only in the Lessini Mountains); 3) pseudonodular and 4) bioclastic limestones of the Bajocian p.p.-Callovian p.p. Rosso Ammonitico Inferiore (RAI); 5) well bedded cherty limestones (Callovian p.p.-Oxfordian p.p. Rosso Ammonitico Medio, RAM and Bathonian p.p.-Kimmeridgian p.p. Fonzaso Formation); 6) nodular limestones of the Kimmeridgian p.p.-Tithonian Rosso Ammonitico Superiore (RAS); 7) micritic cherty limestones of the Lower Cretaceous Maiolica. Compiled based on various sources (e.g., Martire et al. 2006; Préat et al. 2006; Roghi & Romano 2009; Serafini et al. 2022).

levels of oxygenation (e.g., Martire 1996; Massari & Westphal 2011). Sedimentation rates are considered very slow, in the range of a few mm/kyr, even if the reduced thickness of RAV (max 30 m) seems due to strong compaction and frequent and prolonged gaps more than to extremely low sediment accumulation rates (e.g., Martire & Clari 1994). Based

on the interpretation as precessionally-controlled RAV rhythmic nodular-microbial couplets, Massari and Westphal (2011) hypothesized a significantly higher sedimentation rate than the value calculated by Martire & Clari (1994). Being deposited on horst blocks far from the continent and surrounded by deeper basins, the only source of sediments of

RAV was represented by slow pelagic rain plus a certain benthic and nektonic component (Martire et al. 2006). Certain areas of the Trento Plateau and some RAV intervals show sedimentary structures indicating high energy episodes in a background of gentle and more or less constant bottom currents (Massari & Westphal 2011) or, more generally speaking, intermittently active currents (e.g., Martire et al. 2006). Lacking a present-day analogue for the Rosso Ammonitico facies, unambiguous proof of the paleodepth of RAV is so far wanting and literature is divided into "shallow" versus "deep water" factions (e.g., Winterer & Bosellini 1981; Zempolich 1993; Winterer 1998; Massari & Westphal 2011). Such controversy is however quite artificial, as the Rosso Ammonitico facies can form at different bathymetries (e.g., Préat et al. 2011). The presence of microbialites is by no means a proof of RAV shallow water origin (i.e., deposition still located in the photic zone; see Massari & Westphal 2011) because such structures can be produced by a variety of microorganisms (bacteria, archaea and eukaryotes) both in shallow and deep water (except for Cyanobacteria) and therefore they can form regardless of the sunlight (e.g., Winterer 1998; Flugel 2010). Even some RAV sedimentary features, such as sand-size layers with normal grading and planar to hummocky cross bedding, evoked as proxies of "shallow" paleodepth (e.g., Massari 1981; Zempolich 1993; Massari & Westphal 2011), are ambiguous and only diagnostic of the strength and directions of bottom currents because they are known from essentially all depths in the ocean (Winterer 1998). Regardless of various interpretations, it is plausible that RAV was deposited at a few hundred meters depth (i.e., in the upper bathyal zone), the more conservative estimation proposed by Winterer (1998), taking into account a marked variability depending on the area of deposition ("lows" and "highs" generated by block faulting) on the Trento Plateau (Martire 1996).

MATERIAL AND METHODS

Specimens

A total of 23 specimens were included in this study (considering isolated elements as standalone specimens). The dataset (see Table 1) is composed of:

Ichthyosaurs: V7101, V7102, V7158 housed in the Verona Natural History Museum; MCLSC T1 (preliminary number) housed in Museo Civico della Laguna Sud in Chioggia (Venezia).

Thalattosuchians: MGP-PD 26552, MGP-PD 6572 (part), MGP-PD 6761, MGP-PD 27566, MGP-PD 32438 housed in the Museum of Nature and Humankind of the University of Padova; MGGC 8846/1UCC123a, MGGC 8846/1UCC123b and MPPPL 35, MPPPL 39 (all part of the same holotype of *Neptunidraco ammoniticus* in four serial slabs) at the Collezione di Geologia "Museo Giovanni Capellini" of Bologna and at Museo di Paleontologia e Preistoria "Piero Leonardi" of Ferrara; MM 25.5.1078 housed at Museo Padre Aurelio Menin in Chiampo (Vicenza); FOS03839 housed in the Fondazione Museo Civico di Rovereto (Trento); MCLSC T2 (preliminary number) housed in the Museo Civico della Laguna Sud di Chioggia (Venezia).

Plesiosauroids: MGP-PD 6752 (part), MGP-PD 6753, MGP-PD 6754, MGP-PD 6755, MGP-PD 6756, MGP-PD 6757, MGP-PD 6758, MGP-PD 6759, MGP-PD 6760, housed in the Museum of Nature and Humankind of the University of Padova, MPPPL 18797 housed at Museo di Paleontologia e Preistoria "Piero Leonardi" of Ferrara and PLS T1 (preliminary number), non-musealized specimen still located in a seaway dam in Pellestrina (Venezia).

Except for MGP-PD 27566, MPPPL 18797 and MCLSC T1, the specimens have not been prepared.

Tapho-osteological and associated fauna analysis

Skeletal elements of each specimen were measured to the nearest millimeter to estimate the in-vivo size of the animals. Total length was estimated for crocodylomorphs by cranial or femoral length using the equations in Young et al. (2012); for ichthyosaurs, total length was estimated by comparing measurements to more complete specimens of closely related taxa. Mass in ichthyosaurs and plesiosaurs was estimated following the volumetric method using the formula: Mass = volume x 1025 kg/m^3 (density of seawater); Volume= (taxon-specific shape constant x total length)^3; shape constants were derived from Gutarra et al. (2019: ichthyosaurs; 2022: plesiosaurs). The volumetric technique for mass estimation relies on the assumption that marine reptile carcass density is equal to that of seawater. As this assumption appears unlikely to be met (Reisdorf et al. 2012), these should be considered minimum estimates; therefore, estimates of total mass were rounded up to the nearest 10 kg.

Skeletons were subdivided into anatomical units (head, anterior column, posterior column, pectoral girdle-forelimbs, pelvic girdle-hindlimbs; modified after Beardmore et al. 2012) to evaluate their potential displacement relative to the rest of the body and to assess specific taphonomic parameters. Scoring ranged from 0 to 4 (0% = 0; 1-25% = 1; 25-50% = 2; 50-75% = 3; 75-100% = 4; Beardmore et al. 2012; Cleary et al. 2015) to account for: Cp = completeness (scoring for percentage of completeness for each anatomical unit); Ar = articulation

(scoring for percentage of articulation for each anatomical unit); E = erosion (scoring for percentage of eroded compact bone for each anatomical unit).

Pictures of the specimens were taken with either a Canon 700D or a Sony ILCE-7RM3 camera. For most specimens, UV-induced fluorescence was used for the identification of histological and taphonomical details of the skeletal tissue, as well as the discrimination of the associated calcitic fauna from the surrounding matrix. UV-A (peak emission at 368 nm), UV-B (peak emission at 318 nm) and UV-C (peak emission at 254 nm) wavelengths were produced with a 95 W discharge lamp from Way-TooCool LLC.

Associated faunal components were counted from the specimen slabs in the proximity and on the same stratigraphic layer as the remains, but a specific threshold distance from the skeletal material (see Danise et al. 2014) was not set. Following the approach of Maxwell et al. (2022), invertebrate taxa found in the proximity of the remains were considered part of the deadfall if there was direct evidence of encrustation or bioerosion, or if their occurrence is relatively rare in RAV lithologies; in addition to this, common RAV invertebrate taxa were considered as part of the deadfall community if their numbers were exceedingly high (e.g., belemnites).

To evaluate the presence of microbial microborings and the presence of spongiosa-localized pyrite, three histological sections were obtained from MPPPL 18797 (unidentified fragment), V7101 (rib fragment) and MCLSC T1 (vertebral? fragment). Bone fragments were embedded in epoxy resin and cut to 30 μm thick slides. Thin sections were then analyzed with either a SEM Jeol JSM-6010 plus/LA at 20kV, 10 mm WD and with a spot size of 30 nm at the University of Modena and Reggio Emilia or a variable pressure Environmental Scanning Electron Microscopy (ESEM Zeiss EVO MA 15) at the University of Ferrara (Tecnopolo Ferrara).

Micropaleontological analysis

In the framework of previous descriptive studies (Serafini et al. 2020, 2023b) and for novel data, small samples of matrix were extracted from the specimen slabs. From three samples (V7101, V7102, MGP-PD 32438), three 30 μm slices were produced for microfacies analysis. To analyze the calcareous nannofossil content, samples were pro-

cessed according to the smearing technique (Bown & Young 1998) or according to the modified settling technique of Flores and Sierro (1997). Calcareous nannofossil assemblages were semi-quantitatively estimated by counting all the coccoliths and nannoliths recorded in 300 fields of view. Relative species abundances are reported as abundant (A, >1 individual every 1–10 observation fields), common (C, 1 individual every 1–10 observation fields), frequent (F, 1 individual every 10–30 observation fields) and rare (R, 1 individual every > 30 observation fields). Biostratigraphy is described with reference to the biozonation scheme of Casellato (2010). These analyses were performed using a polarized light microscope under a magnification of 1250× at the University of Pavia.

Institutional abbreviations

MGP-PD (Section of Geology and Paleontology of the Museum of Nature and Humankind, University of Padova); MCSNV: Museo Civico di Storia Naturale of Verona; MGGC: Collezione di Geologia (Museo Giovanni Capellini), University of Bologna; MPAMC: Museo Padre Aurelio Menin in Chiampo (Vicenza); Museo Paleontologia e Preistoria "Piero Leonardi" (MPPPL; University of Ferrara); Museo Civico della Laguna Sud di Chioggia (Venezia); MCLSC: Fondazione Museo Civico di Rovereto (FO-MCR, Trento).

Abbreviations of lithostratigraphic names

RAV: Rosso Ammonitico Veronese; RAI: lower member of the Rosso Ammonitico Veronese (Rosso Ammonitico Inferiore); RAM: middle member of the Rosso Ammonitico Veronese (Rosso Ammonitico Medio); RAS: upper member of the Rosso Ammonitico Veronese (Rosso Ammonitico Superiore).

RESULTS

All surveyed RAV specimens are here reported in stratigraphic order (Fig. 1C), with details on their taxonomy, size estimation, horizon, and source locality. The taphonomy of each specimen is also reported, framing the degrees of articulation, completeness, and erosion. If present, associated fauna is listed, together with bite or bioerosion traces. Below, six of the more representative deadfalls were selected for a more extensive description. The remaining specimens are listed in Table 1.

MCLSC T2: Metriorhynchoidea indet. (Thalattosuchia)

Generality – Upper Bajocian metriorhynchoid from the RAI of (most likely) Sasso d'Asiago (Vicenza province), recognized in Pellestrina (Venezia Province) breakwaters in the 1990s. The specimen

Specimen	Taxonomy	Age	Locality and Horizon	Composition	Size	Preservation	Landing	Associated fauna/traces
MCLSC T2 [T1]	Metriorhynchoidea (Thalattosuchia)	middle-late Bajocian	Asiago Plateau, RAI	Dorsal-sacral column, pelvic elements, femur	ETL=3.3m	Sem.art, opisthotonic, eroded elements	Lateral	23 rhyncholites 1 belemnite 117 crinoid
MM 25.5.1078 [T2]	Metriorhynchoidea (Thalattosuchia)	middle-late Bajocian	Asiago Plateau, RAI	Sectioned dentigerous rami, teeth	n.a.	Isolated fragments, eroded bone/enamel	n.a.	Sponge/endolithic fungal borings in bone and teeth
PLS T1 [P1]	Pliosauridae (Plesiosauria)	late Bajocian	Asiago Plateau, RAI	Partial skull, ?mandible, , teeth, vertebrae	n.a.	Flattened eroded skull	Ventral	1 shark tooth 9 rhyncholites 5 belemnites 4 echinoids 5 crinoids
MGGC 8846/1UCC12 3a-b, MPPPL 35-39 [T3]	*Neptunidraco ammoniticus* (Metriorhynchidae, Thalattosuchia)	late Bajocian-early Bathonian	S. Ambrogio di Valpolicella, RAI	Sectioned skull and mandibles, cervical centra	ETL=4.3m	Almost complete and articulated skull, eroded enamel	n.a.	7 rhyncholites 2 *Laevaptychus* 1 *Lamellaptychus* 78 belemnites 92 crinoids
MGP-PD 32438 [T4]	Metriorhynchidae (Thalattosuchia)	late Bajocian-late Bathonian	Cima del Porco, Asiago Plateau, RAI	Partial skull roof, mandibles, cervical centra/ribs, 1 tooth	ETL=2.7m	Cranial imprints, flattened eroded skull, sem.art. column	Dorsal	4 rhyncholites 2 *Laevaptychus* 1 *Lamellaptychus* 5 belemnites 3 crinoids
FOS03839 [T5]	Metriorhynchoidea (Thalattosuchia)	late Bajocian-Callovian	Valbella, Asiago Plateau, RAI	Sectioned dentigerous rami, teeth	n.a.	Isolated fragments, bone tissue well preserved	n.a.	Microbialites
MPPPL 18797 [P2]	*Anguanax zignoi* (Pliosauridae, Plesiosauria)	early-middle Oxfordian	Kaberlaba, Asiago Plateau, RAM	Partial skull, mandibles column, left propodials-epipodials	ETL=3-4m	Flattened, heavily eroded elements	Lateral?	5 shark teeth 16 rhyncholites 17 echinoids 1 *Lamellaptychus* 596 crinoids
MGP-PD 26552 [T6]	"*Steneosaurus*" barettoni (Thalattosuchia)	middle-late Oxfordian	Treschè, Asiago Plateau, RAS	Partial skull roof, mandibles, teeth	ETL=3.7m	Rostral imprint, flattened eroded skull, art.mandibles,	Ventral	8 rhyncholites 1 *Lamellaptychus* 2 crinoids
MGP-PD 6752 part*, 6761 [S1]	Sauropsida indet.	latest Oxfordian-Kimmeridgian	Cesuna, Asiago Plateau, RAS	2 isolated contiguous centra.	n.a.	Loose elements	n.a.	Shark bite on 6761 centrum
MGP-PD 6753 6757, 6758, 6759, 6760 [P3]	Plesiosauria indet.	latest Oxfordian-Kimmeridgian	Cesuna, Asiago Plateau, RAS	5 isolated centra	n.a.	Loose elements	n.a.	2 crinoids on 6757 and 6759 matrices
MGP-PD 6752 part*, 6756, 6754, 6755 [P3]	Plesiosauria indet.	latest Oxfordian-Kimmeridgian	Cesuna, Asiago Plateau, RAS	4 isolated neural arches	n.a.	Loose elements	n.a.	None
V7101 [IT1]	?Ophthalmosauria (Ichthyosauria)	early Kimmeridgian	Monte Interrotto, Asiago Plateau, RAS	Partial column with ribs, pectoral girdle elements	ETL=3-3.5 m	Flattened, heavily eroded elements	Lateral/anterior	2 shark teeth 1 reptile tooth 3 rhyncholites 7 *Laevaptychus* 3 *Lamellaptychus*
V7102 [IT2]	Ichthyosauria indet.	early Kimmeridgian	Monte Interrotto, Asiago Plateau, RAS	Partial anterior column with ribs	?	Sem.art column, flattened ribs	Lateral	None
MCLSC T1 [IT3]	Ophthalmosauria (Ichthyosauria)	Kimmeridgian	Asiago Plateau, RAS	Partial skull, mandibles, cervical centra	?	Disarticulated	Anterior	26 rhyncholites 2 belemnites 3 *Lamellaptychus* 6 *Laevaptychus* 2 crinoids 4 clavate erosions
MGP-PD 27566 [T7]	Aeolodontinii indet. (Thalattosuchia)	latest Kimmeridgian-earliest Tithonian	Ponte Serra, Belluno RAS	Thoracic, sacral and caudal vertebrae, ribs/gastralia, ischium, osteoderms	1.5 m?	Regurgitalite	Clustered mass	Possible bone elements of other ingested taxon
V7158 [IT4]	Thunnosauria indet. (Ichthyosauria)	early Tithonian	Erbezzo, Verona, RAS	Rostrum tip	n.a.	Loose broken rostrum tip	n.a.	Echinoid-like grazing traces

Tab. 1 - Surveyed specimens dataset. Abbreviations: ETL, estimated total length; sem. art, semiarticulated; art, articulated. *the specimen MGP-PD 6752 is an artificial composite of plesiosauroid neural arch and undetermined sauropsid centrum (see Serafini et al. 2023b).

consists of a partial and articulated vertebral column, one femur and portions of the pelvic and ?pectoral girdles (ischium, pubis and a dubious coracoid) on a RAV boulder (Fig. 2A, B; for detailed anatomical description see Serafini et al. 2023b). The specimen was not prepared. Estimated total length: about 3.3 m. Estimated mass: not available.

Taphonomy and preservation – The taphonomy of this specimen is reported in Serafini et al. (2023b), where MCLSC T2 is described as laterally oriented on the surface of a RAV boulder, distinctively arched dorsally in an opisthotonic position (Fig. 2B). Completeness and articulation are low in the anterior column (Cp=1; Ar=2), anterior girdles-forelimbs (Cp=0; Ar=0/4), and posterior girdles-hindlimbs (Cp=2; Ar=0), but relatively higher in the posterior column (Cp=2; Ar=4). Most of the ribs are not preserved, as well as other small and thin elements (e.g., epipodials); this condition is inconsistent with the action of bottom currents, as centra, the femur and pelvic elements would have been scattered. Every preserved anatomical unit is uniformly heavily erod-
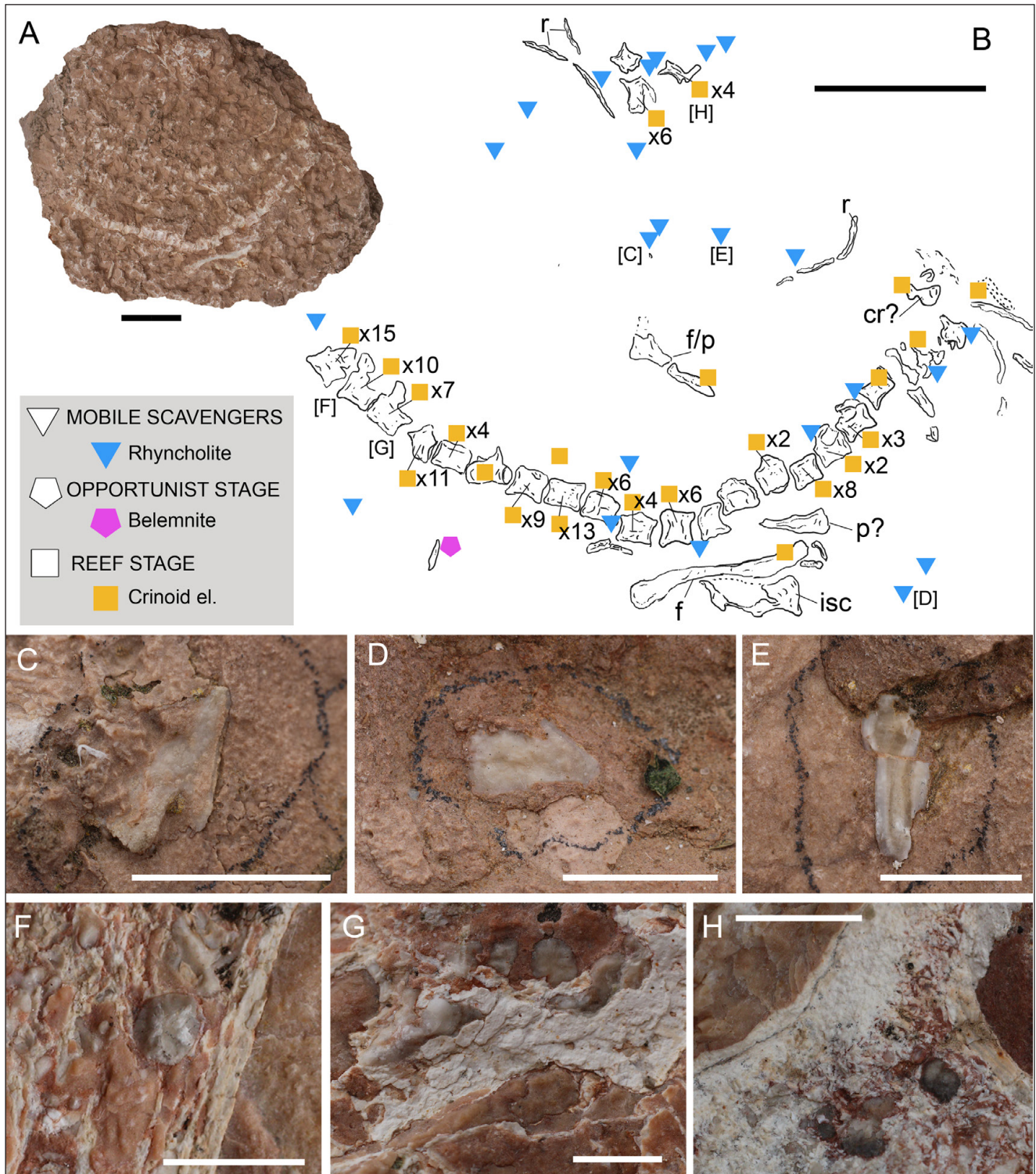
Fig. 2 - Associated fauna of MCLSC T2 (Metriorhynchoidea indet). A) Overview of the RAV block with the specimen. B) Anatomical drawing of the specimen with detail of the associated fauna. C-E) Close-ups of rhyncholites found in close association with the skeletal elements. F-H) Crinoidal elements embedded in MCLSC T2 vertebral cancellous bone. Panel positions correspond to letters in brackets. Abbreviations: cr, coracoid; el., element; f, femur; isc, ischium; p, pubis; r, rib. Scale bars: A, B) 20 cm; C) 2 cm; D, E) 1 cm; F-H) 0.5 cm.

ed (E=4), with widespread exposed cancellous bone. The paucity of elements prevented speculation on the landing of the carcass on the seafloor, but (assuming the boulder surface to match the polarity of the stratum) it eventually settled on the left side (Fig. 2B).

Associated fauna – Abundant nautiloid rhyncholites (n=23, both *Gonatocheilus* and *Leptocheilus*-like

morphotypes; Fig. 2B–E) and a single belemnite rostrum are preserved in close proximity of the skeletal remains. Tens of crinoid elements (n=117) encrust most of the vertebrae. Stalk or holdfast fragments are found deeply embedded between the trabeculae as gray circular objects (Fig. 2B, F–H), slightly raised from the surrounding bone tissue. Despite most of the articula lacking diagnostic features, some are consistent with Phyllocrinidae (Hess 2012), already reported in RAV lithologies (e.g., Clari et al. 1990; Laub 1994). While the presence of the single belemnite rostrum can be considered co-incidental, both rhyncholites and crinoids are here recognized as part of the metriorhynchoid deadfall (see discussion below on fall stage attribution).

PLS T1: Pliosauridae indet. (Plesiosauria)

Generality – Upper Bajocian pliosaurid plesiosaurian from the RAI of (most likely) Sasso d'Asiago, Asiago Plateau (Vicenza province), recognized in 2008 on a boulder used in the breakwater of Pellestrina (Venezia). The specimen was found on a RAV boulder situated in a seaway dam in Pellestrina (Venezia Lagoon) where it currently still resides. A preliminary report was made by Cau & Bizzarini (2020), who attributed the specimen to Pliosauridae pending extraction and preparation. We surveyed the boulder *in situ* and for the first time we provide its datation by means of calcareous nannofossil analysis. The specimen consists of a partial skull roof in dorsal view, three dislodged teeth, an isolated vertebra and neural arch, a ?mandible, and several unidentified and eroded fragments on a RAV boulder (Fig. 3A, B). Estimated total length: not available. Estimated mass: not available.

Age determination – The calcareous nannofossil assemblage, moderately preserved and diversified, is composed of *Watznaueria* aff. *W. manivitae* Bukry, 1973 (C), *W. communis* Reinhardt, 1964 (R), *W. manivitae* (R), *W. britannica* (Stradner, 1963) Reinhardt, 1964 (R), *W.* aff. *W. britannica* (R), *W. gaetanii* Erba in Visentin et al., 2023 (R), *W. contracta* (Bown & Cooper, 1989) Cobianchi et al., 1992 (R), *Cyclagelosphaera margerelii* Noël, 1965 (R), *Lotharingius velatus* Bown & Cooper, 1989 (R). The presence of *W. manivitae* and the absence of *Carinolithus superbus* (Deflandre in Deflandre & Fert, 1954) Prins in Grün et al., 1974 and *Watznaueria barnesiae* (Black in Black & Barnes, 1959) Perch-Nielsen, 1968 allow the sample to be ascribed to the upper Bajocian subzone NJT10b (Casellato 2010) (Fig. 1C).

Taphonomy and preservation – Most of the skeletal material is lost, either as a consequence of the taphonomic history of PLS T1 or due to recent weathering by the sea (the boulder is a few centimeters from the water). With this ambiguity, articulation, completeness, and erosion parameters lose significance. Histologically, the skeletal tissue is represented only by cancellous bone, while the tooth enamel, although cracked and flaked, is still preserved above the dentine. If the boulder surface matches the upper polarity of the stratum, we can infer that the specimen, at least the head, landed and settled ventrally (Fig. 3B).

Associated fauna – Surprisingly, PLS T1 still hosts a relatively diverse associated fossil fauna (Fig. 3C–H): nine rhyncholites (the most complete being *Gonatocheilus*-like) were found on the boulder close to the skeletal material, one of which is stuck between the lateral margin of the left frontal (Fig. 3B, D). Five belemnites are present in the proximity of the remaining bones and 4 crinoid elements were found embedded in the skull (Fig. 3B, G). Echinoid spines are also present (n=4) next to the skull roof, ?mandible and vertebra (Fig. 3B, F). Most interestingly, a shark tooth was found below the isolated rib: only the tip of the crown is preserved (Fig. 3B, C), hampering taxonomic attribution. As with the pliosaur teeth, the shark tooth enameloid is well preserved.

MGGC 8846/1UCC123a, MGGC 8846/1UCC123b, MPPPL 35, MPPPL 39: *Neptunidraco ammoniticus* (Thalattosuchia)

Generality – Upper Bajocian-lower Bathonian metriorhynchid from the RAI of S. Ambrogio di Valpolicella (Verona province), found in Portomaggiore in 1955. The specimen consists of a partial skull, mandibles, and cervical vertebrae on four different sectioned and polished slabs of RAV (Fig. 4A). All slabs together represent the holotype and the only known specimen of the species *Neptunidraco ammoniticus* Cau & Fanti, 2011. Besides polishing, the specimen was not prepared. Estimated total length: 4.3 m. Estimated mass: 340 kg, calculated based on estimates for *Metriorhynchus* spp. published by Foffa et al. (2014: supplement).

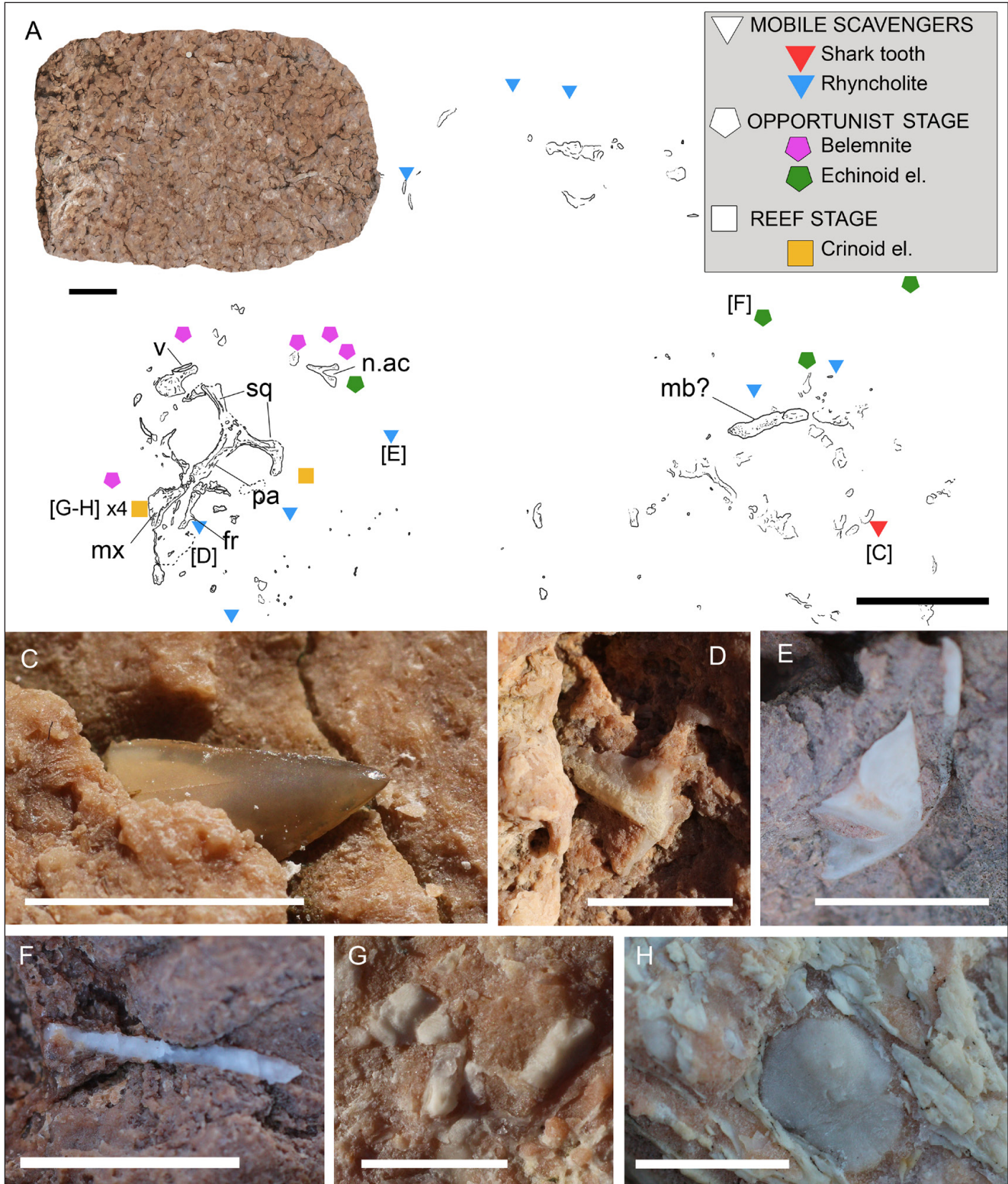*Taphonomy and preservation* – Most of the taphonomic survey on the specimen was carried out on

Fig. 3 - Associated fauna of PLS T1 (Pliosauridae indet.). A) Overview of the RAV block with the specimen. B) Anatomical drawing of the specimen with detail of the associated fauna. C) Shark tooth crown found near the ?mandible. D) Rhyncholite found embedded in the specimen left frontal. E) Associated rhyncholite. F) Echinoid spine. G, H) Crinoid elements embedded in the cranial cancellous bone. Panel positions correspond to letters in brackets. Abbreviations: el., element; fr, frontal; mb, mandible; mx, maxilla; n.ac, neural arch; pa, parietal; sq, squamosal; v, vertebra. Scale bars: A,B) 20 cm; C, D, G, H) 0.5 cm; E) 2 cm; F) 1 cm.

MGGC 8846/1UCC123a and MPPPL 35 exposed sides (Fig. 4A, B), being the two slabs with more preserved skeletal elements. The anatomical unit of the head scores high values of completeness (Cp=3)
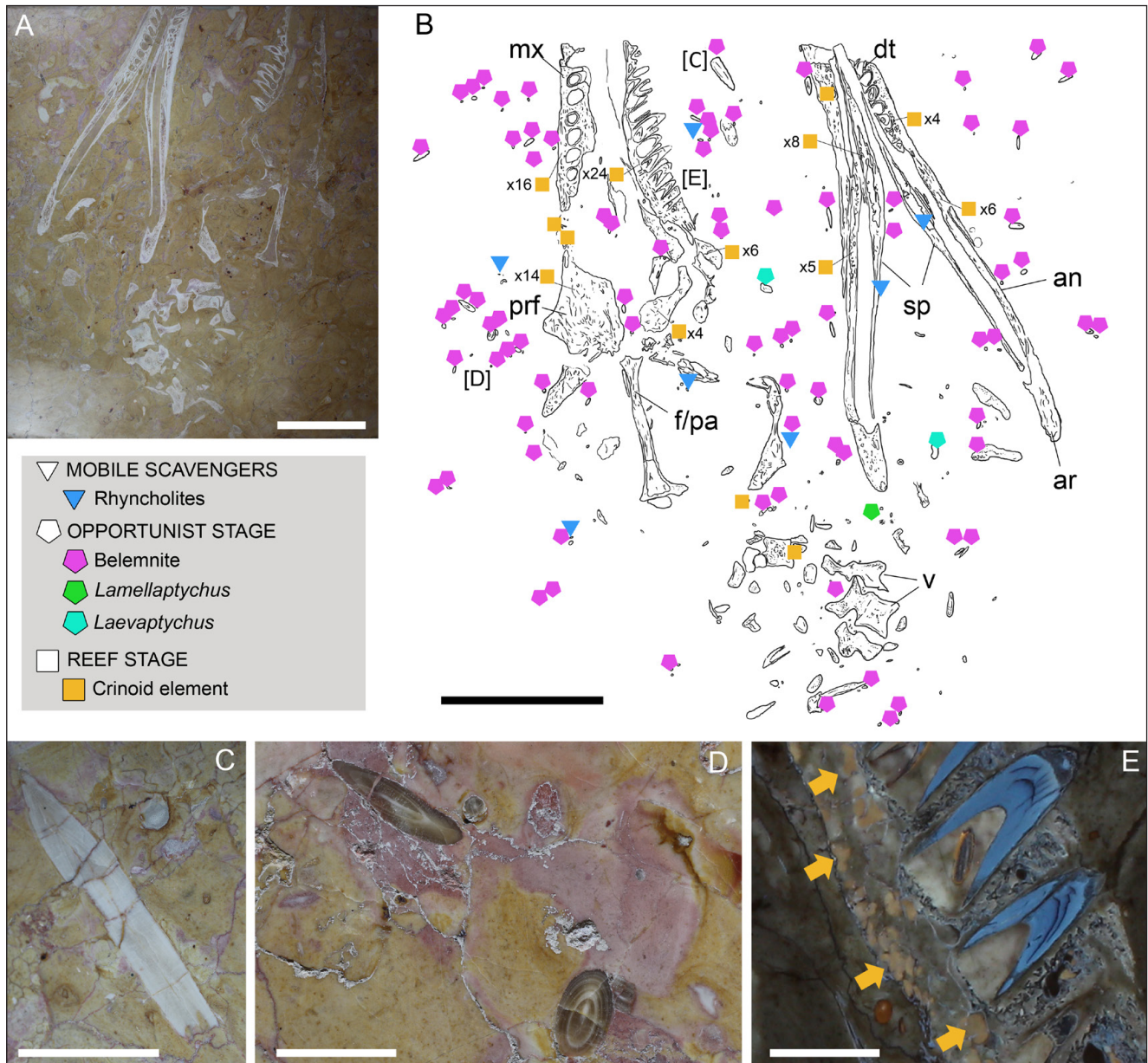
Fig. 4 - Associated fauna of the *Neptunidraco ammoniticus* holotype. A) Overview of the RAV slab with the specimen (MPPPL 35). B) Anatomical drawing of the specimen (from MGGC 8846/1UCC123a) with detail of the associated fauna. C, D) Selected belemnites in close proximity of the skull. E) Sectioned maxillary teeth under UV-ABC with details of crinoid colonization (arrowed) and preferential preservation of enamel only in replacement tooth crowns. Panel positions correspond to letters in brackets. Abbreviations: an, angular; ar, articular; dt, dentary; f/pa, fronto-parietal bar; mx, maxilla; prf; prefrontal; v, vertebra. Scale bars: A, B) 20 cm; C) 5 cm; D, E) 2 cm.

and articulation (Ar=3), with connected sutured bone and with mandibular rami in anatomical association. The anterior column is poorly represented (Cp=1) yet discretely articulated (Ar=2). This degree of articulation of the preserved elements indicates little disturbance at the seafloor. Since the specimen is two-dimensionally exposed, erosion cannot be evaluated, but, as for MM 25.5.1078, UV-ABC induced fluorescence highlights enamel-specific response only in a few replacement crowns,

implying chemical dissolution at the water-sediment interface (Serafini et al. 2023b). The paucity of elements, together with the ambiguous polarity of the polished slab, prevent a univocal determination of the carcass landing at the seafloor (either dorsal or ventral).

Associated fauna – The holotype of *N. ammoniticus* is by far the RAV tetrapod with the highest number of associated belemnite rostra (n=78, *Hibolites;* Fig. 4B–D); most of them are consistent in-

size and without any preferential orientation (which supports a low influence of currents at the seafloor). Belemnites are generally common in RAV lithologies (Sarti 1993; Martire et al. 2006), but such an abundance has to be considered unusual, and is here interpreted as linked to the carcass ecological succession (see discussion below). Between the mandibular and maxillary rami, numerous crinoid elements (n=92, likely underestimated, as counted on a single slab) can be seen exclusively under UV radiation (Fig. 4B, E). These crinoid elements were reported as unidentified calcitic spheres by Serafini et al. (2023b). Rhyncholites are also present (n=7), although the cut of the slab prevents full observation of their morphology. Finally, three ammonite aptychi occur in the proximity of the cranium (two *Laevaptychus* and one *Lamellaptychus*). Ammonite internal molds were not considered to be associated fauna, as they are principal components of the RAV lithologies.

MPPPL 18797: *Anguanax zignoi* (Plesiosauria)

Generality – Oxfordian pliosaurid plesiosaur from the RAM of Kaberlaba, Asiago Plateau (Vicenza province), found in the 1980s. The specimen consists of a partial skull and mandibles, isolated teeth, cervical, dorsal, and caudal vertebrae, the right scapulocoracoid, femur, epipodials and isolated metapodials (Figs. 5, 6A) on multiple RAV pieces (Cau & Fanti 2014). MPPPL 18797 is the holotype of the species *Anguanax zignoi* Cau & Fanti, 2016. The specimen was prepared in the 1980s, with some elements being chiseled from the matrix and with the application of glue and cement. For the first time we provide here the precise dating of the specimen by means of calcareous nannofossil analysis. Estimated total length: 3-4 m (Cau & Fanti 2014). Estimated mass: 340-800 kg, based on a similar body shape to that of *Peloneustes* (Guttara et al. 2022: supplementary data).

Age determination – The taxonomic composition of calcareous nannofossil assemblages from the sample consists of moderate to poorly preserved specimens of *Watznaueria* aff. *W. manivitae* (C), *W. barnesiae* (R), *W. britannica* (F), *W. manivitae* (F), *W. communis* (R), *C. margerelii* (R), *D. lehmanii* Noël, 1965 (R), *Lotharingius hauffi* Grün and Zweili in Grün et al., 1974 (R), *L. sigillatus* (Stradner, 1961) Prins in Grün et al., 1974 (R). Based on the absence

of *Cyclagelosphaera wiedmanni* Reale & Monechi, 1994 and the occurrence of both *Lotharingius hauffii* and *L. sigillatus*, the sample can be assigned to the lower Oxfordian subzone NJT13a (Casellato 2010) (Fig. 1C).

Taphonomy and preservation – The *Anguanax* holotype is preserved in numerous different fragmentary slabs that are difficult to re-organize in their original position (Cau & Fanti 2014; 2016 attempted reconstruction of some appendicular element-bearing pieces); for this reason, a complete and accurate assessment of the skeleton articulation is unreliable. The head unit is modestly complete (Cp=2, missing the anterior half of the rostrum and most of the skull roof) but relatively articulated, with only the right mandibular ramus being displaced in a separate fragment (Fig. 5A); only one tooth is found *in situ*, while the closest to the anatomical position are found in the counterside of the loose mandible (Fig. 5E). The pectoral girdle and forelimbs unit is represented by the left scapulocoracoid (Cau & Fanti 2016) and only by one partial humerus (left) with associated epipodial elements. Only the left femur, possible pelvic element fragments and pedal phalanges represent the hind limb-pelvic girdle unit (Cau & Fanti 2014). While the anterior column preserves few disconnected cervical and dorsal vertebrae, the posterior unit is relatively more complete and articulated by means of a large block containing the partial caudal series, with still-associated neural spines and chevrons (Fig. 5C). This block is peculiarly facing the right-side judging from the orientation of the neural spines and arches (Cau & Fanti 2014); this is inconsistent with most of the skeleton lying on the right-side. It is unclear if the column segment detached and rolled into a separate position (possibly due to scavenging; see evidence below) or if it is outcropping (or was prepared) from the underside. Erosion is consistently high throughout the skeleton (E=4), with only few shreds of compact bone remaining (e.g., coracoid surface). Teeth are surprisingly well preserved in their histological structure, with preserved enamel and dentine, largely intact crowns, and well-defined apical ornamentation (Fig. 5E, F). UV-induced fluorescence of the bones is moderate, possibly indicating partial silicification of the original apatite lattice (Fig. 5A, C, E, F). In comparison, calcitic elements of the invertebrate fauna are much more reactive under ultraviolet light (Fig. 5B). The
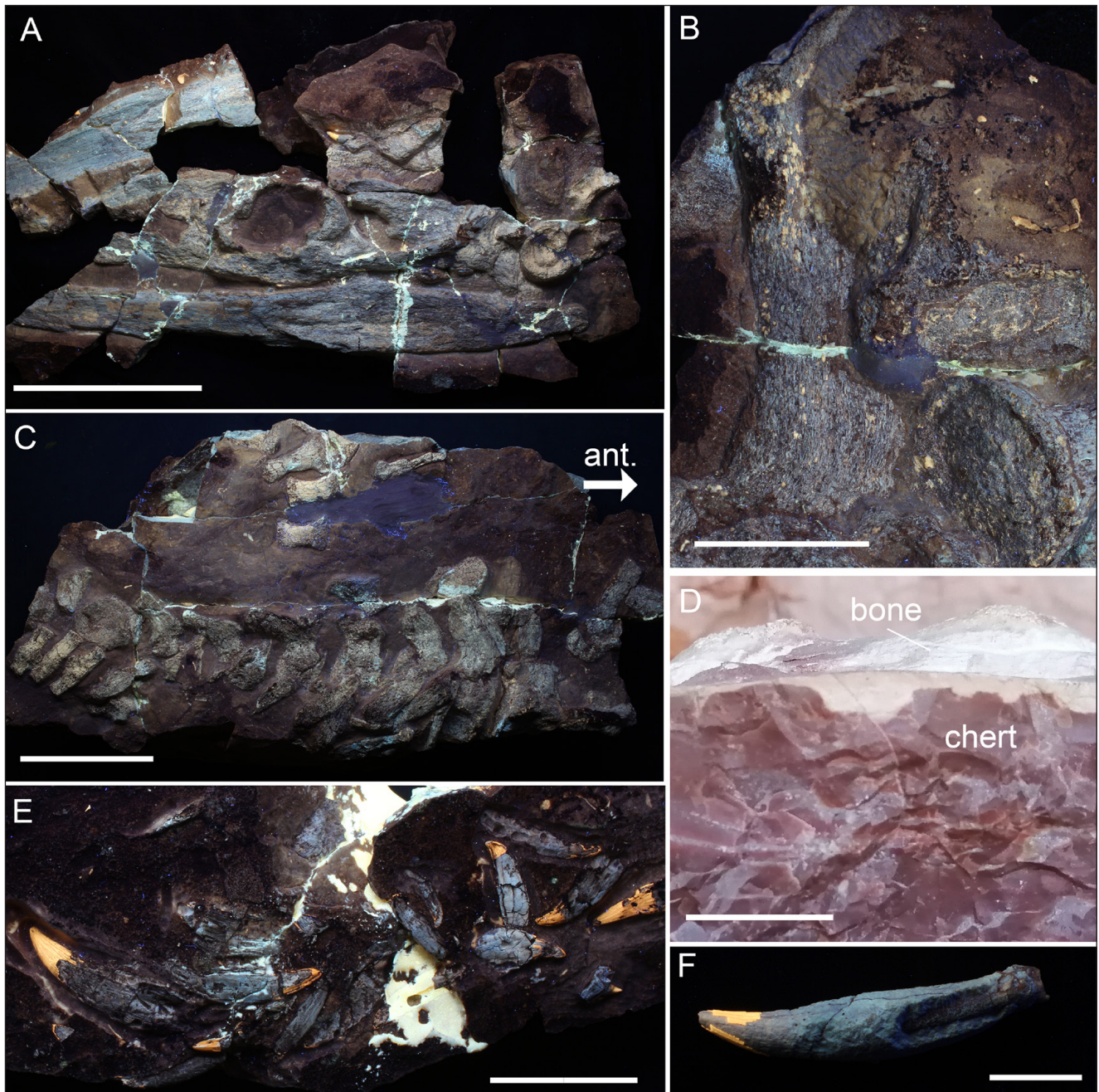
Fig. 5 - Taphonomy of MPPPL 18797 (*Anguanax zignoi*). A) Skull of *Anguanax zignoi* under UV-ABC light. B) Axial and appendicular elements severely affected by crinoid colonization under UV-ABC. C) Articulated caudal column under UV-ABC. D) Bone-chert interface at the border of the slab. E) Teeth under UV-ABC with detail of the enamel preservation. F) Isolated tooth under UV-ABC with detail of the silica infilling of the root. Scale bars: A) 20 cm; B) 10 cm; C) 5 cm; D) 3 cm; E, F) 1 cm.

presence of Si on the bone tissue is also supported by SEM-EDS analysis, and silica infilling can also be observed in the roots of some teeth. SEM analysis on the 3D vertebral fragments did not reveal the presence of pyrite framboids; despite sulfur and iron peaks having been detected with EDS (File S1), distinct crystalline agglomerates of pyrite were not morphologically recognized inside the spongiosa. The same result occurred with the optical analysis of the histological thin section. From SEM imaging, microborings can however be recognized in the trabecular surface (File S1).

Associated fauna – MPPPL 18797 is the RAV deadfall so far recovered with the most abundant associated fauna (Fig. 6). Identification of the calcitic associated fauna was conducted under UV light, as it is almost impossible to distinguish calcitic elements in the red matrix and white bone under nat-
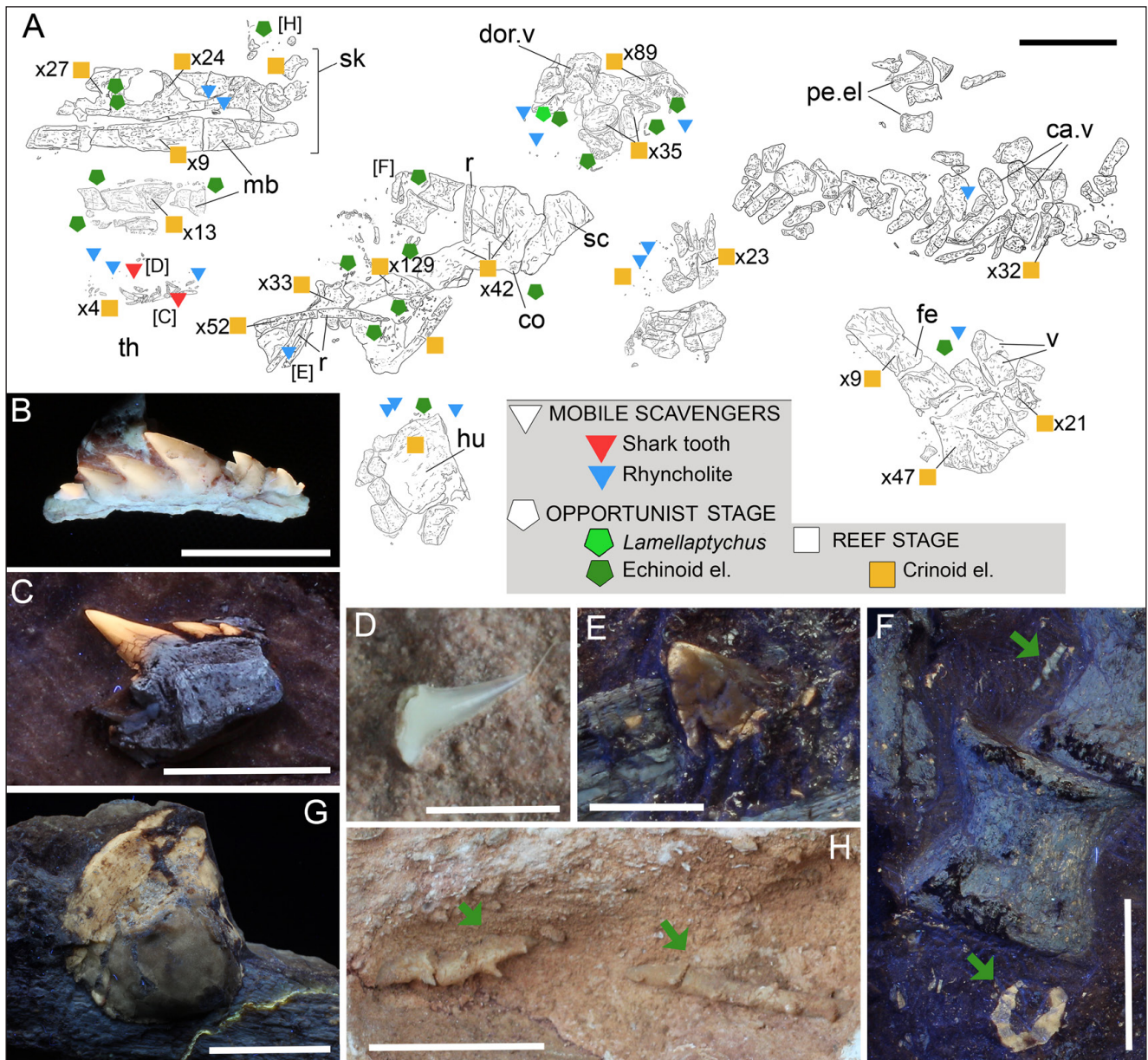
Fig. 6 - Associated fauna of MPPPL 18797 (*Anguanax zignoi*). A) Anatomical drawing of the specimen with detail of the associated fauna. B) Hexanchiform tooth extracted from the specimen. C) cf. *Pseudonotidanus* tooth found close to the pliosaur mandibular ramus. D) *Sphenodus* tooth found close to the pliosaur mandibular ramus. E) Rhyncholite stuck in one of the specimen's ribs. F) Echinoid plate and spine (green arrows) closely associated with the vertebral centra. G) Unidentified bivalve encrusting a bone fragment. H) Echinoid spine with distinctive thorns (green arrows) embedded dorsally to the skull roof of the specimen. B, C, E, F, G are figured under UV-ABC light. Panel positions correspond to letters in brackets. Abbreviations: ca.v, caudal vertebrae; co, coracoid; dor., dorsal vertebrae; el., element; fe, femur; hu, humerus; mb, mandible; pe.el, pedal elements; r, rib; sc, scapulocoracoid; sk, skull; th, teeth; v, vertebrae. Scale bars: A) 20 cm; B, C, E, G, H) 1 cm; D) 2 mm; F) 5 cm.

ural light. The specimen preserves two shark teeth underneath the right mandible (Fig. 6A, C, D); one small crown is consistent in morphology with an upper lateral tooth of *Sphenodus* sp. (Fig. 6D). The cusp is slender and very pointed, bent distally. The labial face is convex transversely, especially in its central region, almost forming a crest. The cutting edges are very acute and prominent, extended laterally by short oblique heels. Characters correspond to the generic description provided by Cappetta (2012: p. 100). The other tooth is larger and more intact (Fig. 6C) and belongs to cf. *Pseudonotidanus* sp. (ca. 1.1 to 1.6 cm wide). Three additional hexanchiform teeth were retrieved and extracted from the carcass as isolated crowns or cusps that are seemingly referable to the same taxon (e.g. Fig. 6B). The cusp is labio-lingually compressed, not curved lingually and devoid of any ornamentation. The crown does not

overhang the root labially. The teeth are strongly asymmetrical, suggesting an anterior position (the tooth with a nearly erect main cusp) and a lateral position (the one with a strongly inclined and slightly sigmoidal main cusp) in the jaw. The main cusp is rather broad, triangular and bent distally. The heels are well-developed and bear numerous mesial and distal cusplets, lower than the main cusp, with the mesial cusplets well separated from the main cusp. Distal cusplets are more developed than the mesial ones. All cusplets are sharp and separated one from the other by deep and sharp notches. Cutting edges are well developed and continuous. The root is pseudopolyaulacorhize and moderately thick when preserved (see the larger tooth underneath the right *Anguanax* mandible). There is a robust lingual bulge and some irregularly spaced foramina, with faint vertical folds separating them. The characters are almost consistent with the description provided by Cappetta (2012: p. 104) for *Pseudonotidanus* teeth; the stratigraphic distribution is also consistent (Toarcian-Oxfordian; Cappetta 2012). 16 rhyncholites are found dispersed in most of the surveyed blocks (Fig. 6A), one of which (*Gonatochelius*-like) still contacts the distal end of a rib (Fig. 6E). 1 *Lamellaptychus* was identified, but more (also *Laevaptychus*) could be represented by smaller sections embedded in the sediment. 17 echinoid elements were observed on MPPPL 18797 between spines and plates (Fig. 6A, F, H); one of the more complete spines found in a notch dorsal to the posterior end of the skull shows distinct thorns on the shaft (Fig. 6H). MPPPL 18797 stands out for the extreme abundance of crinoid articula embedded in the cancellous bone, with 596 counted elements. All the brightly yellow-fluorescent circular or pentagonal objects found in the matrix, on the bones, and between trabeculae were identified as crinoid elements (Figs. 5B; 6F). An unidentified bivalve was also found encrusting an isolated bone fragment (Fig. 6G).

MCLSC T1: Ophthalmosauria indet. (Ichthyosauria)

Generality – Kimmeridgian ophthalmosaurian ichthyosaur from the RAS of (most likely) Sasso d'Asiago, Asiago Plateau (Vicenza province), recognized in 1997 in the breakwaters of Pellestrina (Venezia). Besides a brief report by Bizzarini (2003), the specimen still lacks an official description (and a catalog number), so we briefly discuss its anatomy and taxonomic affinities herein to better frame its taphonomy. As with MCLSC T2 and PLS T1, MCLSC T1 was found in a seaway dam in Pellestrina (Venezia Lagoon) on a RAV boulder quarried from the Asiago Plateau (Bizzarini 2003). The specimen is composed of the partial cranium in ventral view and anteriormost elements of the axial skeleton (Fig. 7). Estimated total length: ~3.6 m total length (~510 kg), estimated based on similarities in parabasisphenoid size and general morphology to *Gengasaurus* and ophthalmosaurines, however a proportionately larger skull relative to the body, as in many platypterygiines, yields total length estimates centered around 2.5–2.9 m.

Skull – The preserved skull roof consists of one postorbital, one postfrontal, the two supratemporals and a single parietal that might include a frontal contribution (Fig. 7B–E, G). The left supratemporal is the best preserved of the pair; it is preserved in dorsal view and appears robust and thickened medially (Fig. 7E). The parietal presents a long, slender supratemporal process and borders a distinctly oval parietal foramen (Fig. 7D). The palatal series is represented by an isolated pterygoid underneath the right supratemporal (Fig. 7C). A large, flat, isolated bone above the mandibles might be interpreted as a palatine (left?; Fig. 7C), but its preservation hampers a definitive identification. The chondrocranium is represented by the parabasisphenoid (PBS) in ventral view (Fig. 7E); this element appears squarish, with broad, anterolaterally directed basipterygoid processes and posteroventrally situated foramen for the internal carotid arteries (ICF). Bizzarini (2003) reports the presence of sclerotic ossicles, and four quadrangular elements still in connection to the right of the parabasisphenoid might be consistent with this interpretation (Fig. 7D).

Mandibles – The lower jaw is mostly represented by the two elongated pairs of angular and surangular bones still close to anatomical association (Fig. 7B). Additional fractured elements are recognizable between the two mandibles (splenials?) but their poor preservation hampers accurate identification (Fig. 7B, G). The anteriormost preserved portion of the rostrum is found isolated in the left bottom corner of the boulder, consistent with both the premaxilla and the dentary (Fig. 7G).

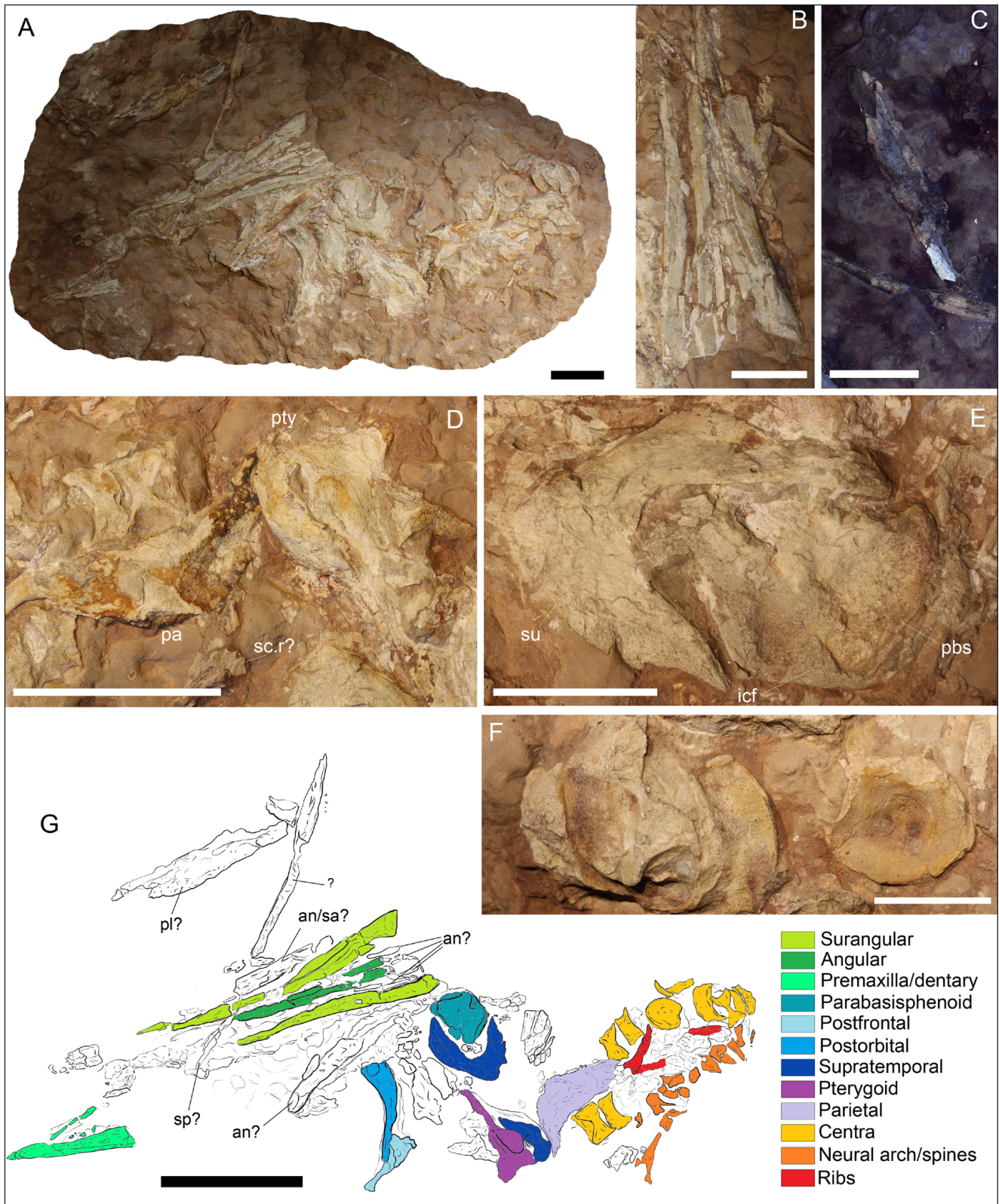*Axial skeleton* – The preserved axial skeleton is comprised of a distinct bone mass separated

Fig. 7 - Overview and anatomical details of MCLSC T1 (Ophthalmosauria indet). A) Overview of the RAV block with the specimen. B) Close-up of the skull in ventral view. C) Close-up under UV-AC light of disarticulated palatal elements. D) Detail of palatal, skull roof and axial elements. E) Parabasisphenoid complex and supratemporal. F) Preserved centra of the specimen. G) Anatomical drawing of the specimen with color differentiation of the cranial and postcranial axial elements. Abbreviations: an, angular; icf, internal carotid foramen, pa, parietal; pbs, parabasisphenoid; pl, palatine; pty, pterygoid; sa, surangular; sc.r, sclerotic ossicles; sp, splenial. Scale bars: A, D) 10 cm; B, C, E) 5 cm; F) 4 cm; G) 20 cm.

from the cranium in the right bottom corner of the boulder (Fig. 7F, G). Ten amphicoelous centra can be identified on the boulder, but several undetermined fragments may also belong to additional vertebrae. About ten, mostly fractured, neural arches and neural spines can be found below the vertebral row, possibly corresponding to the preserved centra. Three fragmentary ribs are also present, with only one displaying a recognizable capitulum as well as a tuberculum of similar size. Judging by size and relative position of the vertebrae and ribs, the vertebral column segment appears to belong to the anteriormost dorsal series.

Taxonomy – No genus-level attribution can be reached due to the paucity and poor preservation of the remains; however, it is noteworthy that the combination of the PBS shape (squarish-subpentagonal; Fig 7E), the posteroventral position of the ICF, the anterolaterally oriented basipterygoid processes and the long and slender supratemporal processes of the parietal (Fig. 7D) is consistent only with *Brachypterygius* and *Gengasaurus* amongst ichthyosaurs from the Kimmeridgian-Tithonian of Europe (Moon & Kirton 2018; Paparella et al. 2017). The following coeval European taxa can be excluded: *Ophthalmosaurus icenicus* Seeley, 1874, *Arthropterygius chrisorum* (Russell, 1993) (different ICF position; Moon & Kirton 2016; Maxwell 2010), *Nannopterygius* spp. (inconsistent PBS and parietal; Zverkov & Jacobs 2021), *Palvennia hoybergeti* Druckenmiller et al., 2012, *Janusaurus lundi* Roberts et al., 2014 (inconsistent parietal)*, Thalassodraco etchesi* Jacobs & Martill, 2020 (body of the parietal subequal to the length of the supratemporal process, vs. much longer in MCLSC T1, Jacobs & Martill 2020), *Undorosaurus gorodischensis* Efimov, 1999 (parietal inconsistent, but PBS identical; Zverkov & Efimov, 2019), *U. kristiansenae* (Druckenmiller et al., 2012) (inconsistent PBS; Delsett et al. 2019). Re-examination of a cast of the neotype o*f Aegirosaurus leptospondylus* (Wagner, 1853) leads us to conclude that the parietal morphology is very similar to that of MCLSC T1, although potentially slightly broader; the PBS of *Aegirosaurus* is unknown. The *Aegirosaurus* neotype is substantially smaller than MCLSC T1. *Gengasaurus* might be a good candidate for referral due to similar PBS morphology, similar body size (based on PBS dimensions) and a sympatric distribution (Paparella et al. 2017); however, the PBS of the holotype and only specimen is not exposed in ventral view. Due

to these uncertainties, MCLSC T1 is here referred to Ophthalmosauria indet., as it was reported in Bizzarini (2003).

Age determination – The calcareous nannofossil assemblage shows high total abundance (more than 3 specimens for each field of view) and moderate preservation. The taxonomic composition is dominated by the *Watznaueria* species that are known as resistant to dissolution. They are *Watznaueria* aff. *W. manivitae* (A), *Watznaueria communis* (C), *Watznaueria manivitae* (large) (C), *Watznaueria* aff. *W. britannica* (C), *Watznauria britannica* (F). Rare specimens of *Cyclagelosphaera margerelii* and rare fragments of *Faviconus multicolumnatus* Bralower et al., 1989 have also been recognized. For the high abundance of *W.* aff. *W. manivitae* and *W. manivitae* (large, > 12 micron) , the occurrence of *F. multicolumnatus* and the absence of *Zeugrhabdotus embergeri* (Noël, 1959) Perch-Nielsen, 1984, the assemblage can be referred to the Kimmeridgian portion of the biozone NJT14 (Fig. 1C).

Taphonomy and preservation – MCLSC T1 scores a medium level of cranial completeness (Cp=2) but is largely disarticulated (Ar=0); the anterior column unit scores similarly (Cp=1; Ar=1), while erosion is equally moderate in all elements (E=2). The landing type of the specimen is difficult to frame due to the paucity and general disarticulation of the remains; the tip of rostrum is broken; no teeth are preserved and the entire preserved skull roof and chondrocranium is disarticulated. We propose that this disposition might be the consequence of a fast anterior landing, with a head-first arrival on the seafloor and possible breakage of the anteriormost rostrum (see Wahl 2009). Histologically, MCLSC T1 is not too poorly preserved, with a large extent of compact bone still intact; however, the skeletal tissues are diagenetically altered: UV-induced fluorescence can help in the distinction of merged skeletal elements, but the response light is weak, possibly due to SiO_2 encrustation (Fig. 7C).

Associated fauna – Twenty-six rhyncholites are found in close proximity of the skeletal remains (Fig. 8A), two of them can be observed piercing the lateral margin of the parabasisphenoid (Fig. 8B, B$_1$). Six laevaptychi and two lamellaptychi are also present (Fig. 8C, D), but most of them are grouped in a slightly more depressed area to the right of the skull, possibly emerging from a lower level of the boulder not synchronous with the ichthyosaur
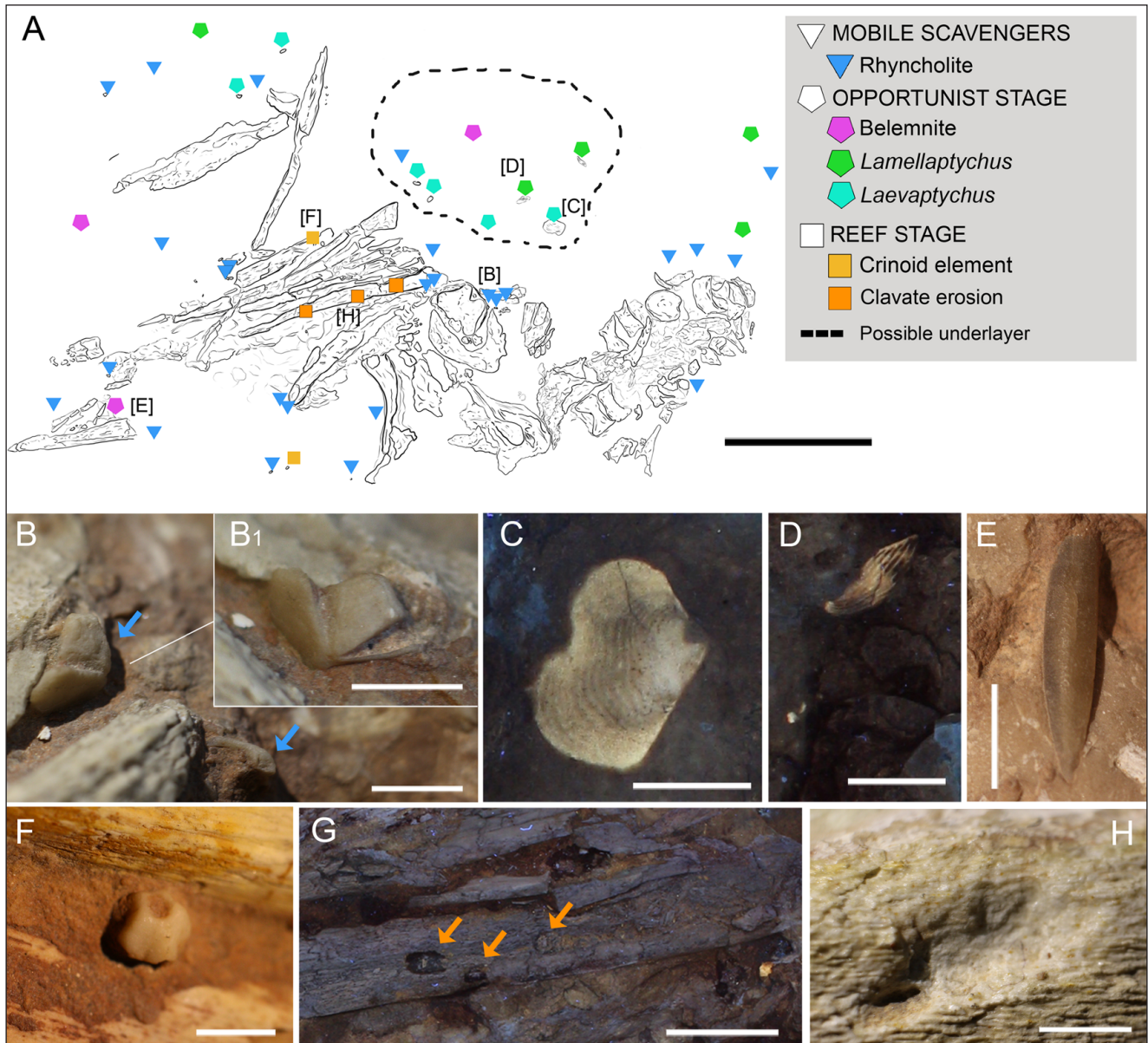
Fig. 8 - Associated fauna of MCLSC T1 (Ophthalmosauria indet). A) Anatomical drawing of the specimen with detail of the associated fauna. B) Rhyncholites piercing the specimen parabasisphenoid, and B$_1$ close-up. C) *Laevaptychus* under UV-ABC light. D) *Lamellaptychus* under UV-ABC light. E) Belemnite closely associated with the anterior end of the rostrum. F) Phyllocrinid calyx found stuck on the left surangular. G) Lower jaw under UV-ABC light to enhance clavate borings (orange arrows). H) Close-up of clavate erosion on the right surangular. Panel positions correspond to letters in brackets. Scale bars: A) 20 cm; B, B$_1$, F, H) 0.5 cm; C, D, E) 1 cm; G) 3 cm.

deposition. Two belemnite rostra (Fig. 8E) and two crinoidal elements also occur, one of which set on the right surangular (Fig. 8F). In addition, subcircular and clavate erosions, possibly attributable to boring bivalves, can be observed aligned on the left surangular (Fig. 8G, H). The histological section produced from a ?vertebral fragment revealed the widespread presence of microborings on most of the trabecular surfaces: borings range from circular to unbranched-elongated, all in the 10-20 μm size range, which is consistent with a bacterial or fungal origin (Trueman & Martill 2002).

V7101: ?Ophthalmosauria indet.
(Ichthyosauria)

Generality – Lower Kimmeridgian ?ophthalmosaurian ichthyosaur from the RAS of Monte Interrotto, Asiago Plateau (Vicenza province). The specimen consists of an articulated vertebral column (anterior dorsal to mid dorsal section), associated ribs, putative unidentified pectoral elements and a possible ischiopubis (Fig. 9A, B). For detailed anatomical and morphometrical description see Serafini et al. (2020). Estimated total length (measured along axial skeleton): 3–3.5 m. Estimat-
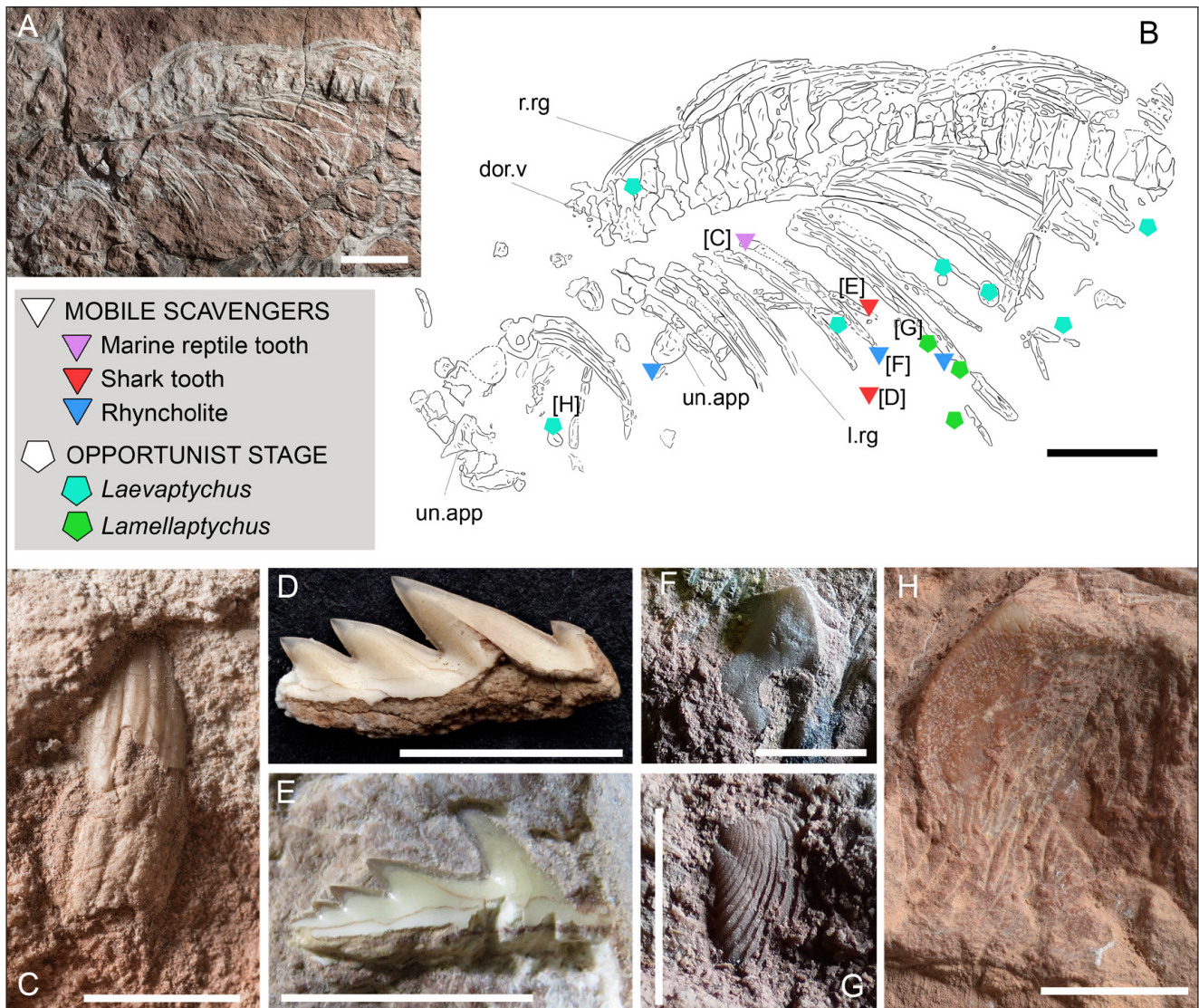
Fig. 9 - Associated fauna of V7101 (?Ophthalmosauria indet.). A) Overview of the RAV slab with the specimen. B) Anatomical drawing of the specimen with detail of the associated fauna. C) Ichthyosaur tooth piercing a rib. D) *Notidanodon* tooth extracted from the slab. E) *In situ Notidanodon* tooth close to the left-side ribcage. F) Close-up view of a rhyncholite found in proximity to the left-side ribcage. G) *Lamellaptychus* found close to the left-side ribcage. H) *Laevaptychus* found in proximity to the anterior end of the specimen. Panel positions correspond to letters in brackets. Abbreviations: dor.v, dorsal vertebrae; l.rg, left-side ribcage; r.rg, right-side ribcage; un.app, unidentified appendicular elements. Scale bars: A, B) 20 cm; C–G) 5 mm; H) 1cm.

ed mass: 300–470 kg, based on an assumed body shape similar to that of *Ophthalmosaurus* (Gutarra et al. 2019).

Taphonomy and preservation – V7101 scores high values of completeness and articulation (Cp=3; Ar=4) only for the anatomical unit of the anterior column, while other preserved elements are too damaged or fragmentary for feasible evaluation. The absence of the skull and girdles-limbs is more consistent with scavenging activity or flotation decay rather than bottom current-scattering, as smaller elements like ribs are still found in anatomical position (Fig. 9B). Except for some poste-

rior centra, almost all skeletal elements of V7101 are heavily eroded to the cancellous bone (E=4). The specimen landing mode could have either been anterior, lateral, or dorsal, but eventually the carcass settled laterally on the right side (Serafini et al. 2020). The specimen then underwent strong lateral lithostatic compression that made its anterior half almost two-dimensional (Serafini et al. 2020).

Associated fauna – V7101 hosts a relatively diverse associated fossil fauna (Fig. 9B–H), with rhyncholites (n=3, all of the *Gonatocheilus*-like morphotype) closely associated with the left side of the ribcage (Fig. 9B, F), *Laevaptychus* aptychi (n=7;
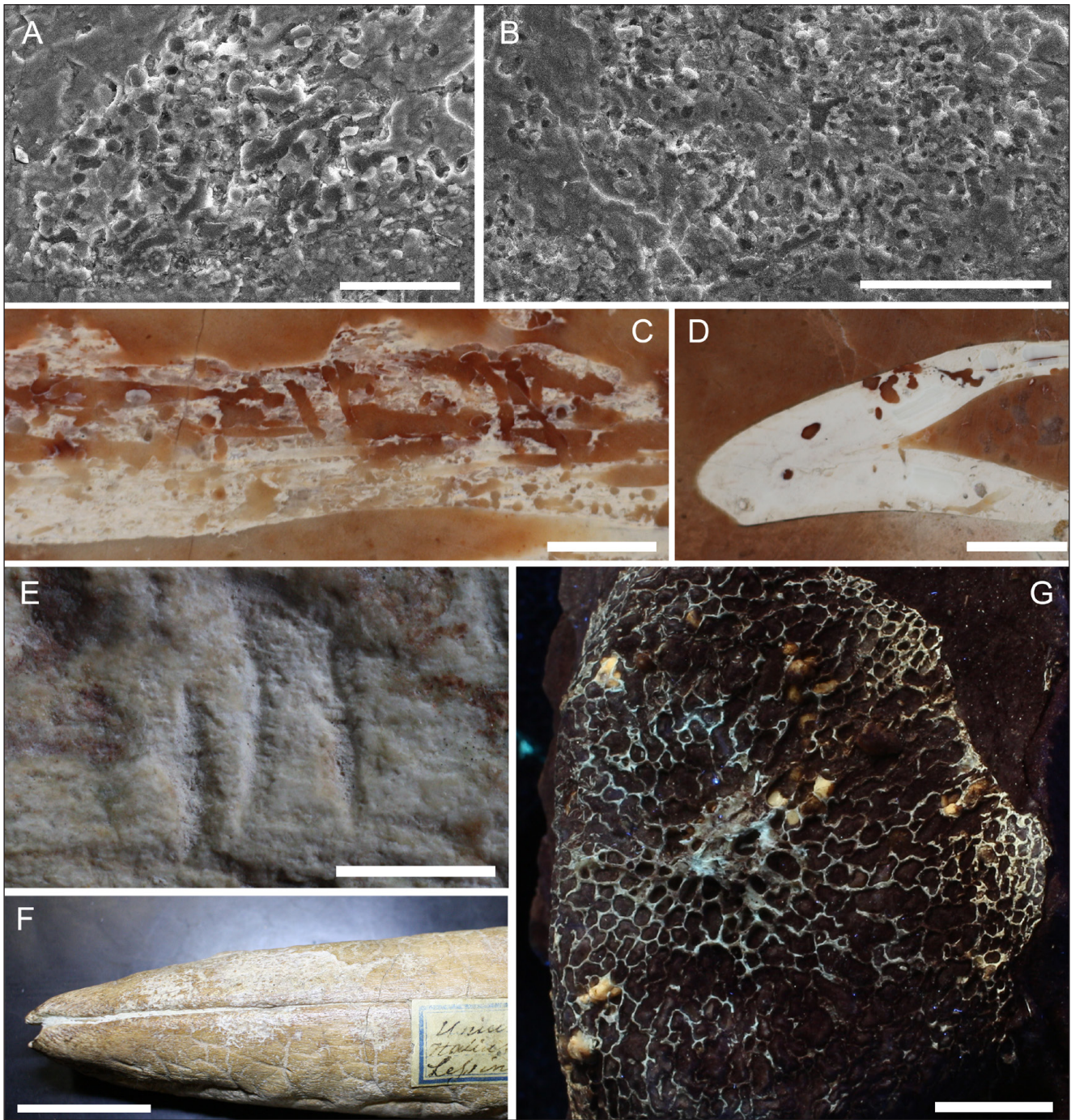
Fig. 10 - Biologically altered skeletal tissues from different specimens. A) Histological section from MCLSC T1 (Ophthalmosauria indet.) under SEM with detail of elongated (possibly fungal) microborings. B) Histological section from V7101 (?Ophthalmosauria indet.) under SEM to illustrate microbial microborings in the trabeculae. C) Unbranched borings in the maxilla of MM 25.5.1078 (Metriorhynchoidea indet.) possibly attributable to sponges. D) Borings in the dentine of an isolated tooth of MM 25.5.1078. E) Possible shark tooth traces on MGP-PD 6761 (Sauropsida indet. centrum). F) Detail of echinoid-like grazing on the surface of V7158 (Thunnosauria indet. rostrum). G) Eroded centrum of MPPPL 18797 (*Anguanax zignoi*) under UV-AC to highlight crinoid growth between trabeculae. Scale bars: A) 100 μm; B) 50 μm; C, D) 5 mm; E, F) 3 cm; G) 1 cm.

Fig. 9B, H), *Lamellaptychus* aptychi (n=3; Fig. 9B, G) in the proximity of the skeleton, two *Notidanodon* shark teeth (Hexanchidae) close to the ribs of the left side of the ribcage (Fig. 9B, D, E), and an ichthyosaur tooth (most likely from a different specimen) still embedded in one of the ribs (Fig. 9C) of the left ribcage (Serafini et al. 2020). As with MCLSC T1 (Fig. 10A), SEM analysis on the histological section revealed the widespread presence of elongated microborings (Fig. 10B).

DISCUSSION

Comparative preservation

With very few exceptions (V7158 and the Cesuna vertebrae; Serafini et al. 2023a, b), all the studied marine tetrapods from the RAV share a poor state of preservation. None is found complete and few preserve at least discretely complete anatomical units. Multiple factors in marine environments affect the completeness of vertebrate carcasses, most notably floating and scavenging (Schmeisser McKean & Gillette 2015). Floating consequent to microbial fermentation and bloating exposes carrion to subaerial decay, whereby weaker anatomical units can detach and disperse far from the body (Schäfer 1972; Shultz et al. 2022). According to previous studies that applied floating models in marine reptiles, this phenomenon would only occur under specific environmental conditions (e.g., high temperature, shallow depth; Reisdorf et al. 2012; Beardmore et al. 2012). These restrictions would seemingly exclude some negatively buoyant taxa (e.g., ichthyosaurs) from having floated up from a deep-water setting such as the RAV; however, we cannot confirm if the surveyed specimens died in their final depositional context or if they were transported by currents from a shallower environment. Therefore, floating cannot be excluded for any RAV specimens. In contrast, we find strong evidence of scavenging, which occurred either during floating or at the seafloor (see discussion below on mobile scavengers).

Overall, the preserved anatomical units are substantially articulated, and where disarticulation occurs (e.g., the anterior centra-ribs of MCLSC T2, skull of MCLSC T1, mandibles and dorsal centra of MGP-PD 32438) loose elements are not scattered across the slabs but instead are found close to their anatomical position and without a preferential orientation. This disposition suggests little disturbance at the seafloor by current activity (Martill 1985; Boessnecker 2014; Bosio et al. 2021), something that has already been hypothesized in various RAV tetrapods studies (Cau & Fanti 2011, 2014; Serafini et al. 2020, 2023b) and is consistent with the low-energy pelagic paleoenvironment that has been proposed elsewhere for the RAV units (Martire 1996; Martire et al. 2006).

The predominance in many specimens of exposed cancellous bone points to erosional processes acting on the bone tissue. Erosive phenomena can be explained by chemical dissolution of the bones above the sediment-water interface during a prolonged exposure of the remains on the seafloor before burial. This process is supported by the extremely slow sedimentation rates hypothesized for the RAV depositional settings (few mm/kyr; Martire et al. 2006). Besides chemical dissolution, large-scale bioerosion of the skeletal tissues might have contributed to the histological degradation (Hedges 2002; Trueman & Martill 2002). Extensive bioerosive phenomena are in fact highlighted in the histological sections, where even small fragments of cancellous bone exhibit dense traces of microbial exploitation (Fig. 10A, B; File S1) as well as larger borings (Fig. 10C, D). Moreover, with greater action of microborers, the dissolution rates in corrosive settings are usually higher (A. Collareta, pers observ). Dental tissues are also affected by superficial erosion. Interestingly, it appears that a preferential dissolution of the enamel occurred in some RAI specimens (all thalattosuchians: MGGC 8846/1UC-C123a, MGGC 8846/1UCC123a-b; MPPPL 35-39, MM 25.5.1078, FOS03839): thanks to UV-induced fluorescence, the enamel response is found absent in the functional crowns of these specimens, while it is present only in some of the replacement teeth still embedded in the alveolus/functional tooth root; Fig. 4E). In the same specimens, dentine and compact/cancellous bone are seemingly intact. Contrarily, in other RAI (PLS T1), RAM (MPPPL 18797) and RAS (MGP-PD 26552, V7101) reptiles, the opposite situation occurs, where tooth enamel and dentine (or enameloid for the associated shark teeth) are preserved (sometimes pristinely) while the bone is critically eroded. Despite being made of the same materials (hydroxyapatite), enamel is structurally very different from other hard tissues in vertebrates, with a very rigid and compact structure of larger apatite crystals, lower collagen content and negligible porosity ('hypermineralized'; e.g., Boyde 1971; Kendall et al. 2018); in this perspective, it is not surprising to identify chemical dissolution phenomena specific to this hard tissue. It is, however, very peculiar to find both the presence and absence of such preferential erosion in the same paleoenvironment. Such specimen-based differences could be related to specific biologically-mediated erosive phenomena (e.g., bacterial or fungal activity; Trueman & Martill 2002).

	Enamel	Dentine/cementum	Compact bone	Cancellous bone	Deformation	UV-fluorescence*	Range	Specimens
TAF-1	Not preserved	Preserved	n.a.**	Preserved	Low or absent	Medium, pale beige-dirty white response color	RAI	T2, T3, T5
TAF-2	Well preserved	Preserved	Highly eroded	Recognizable	Low	Strong, orange response color	RAI-RAS	P1, T6
TAF-3	Well preserved	Eroded	Severely eroded	Collapsed	Strong (2D)	Strong, light blue response color	RAM-RAS	P2, IT1, IT2
TAF-4	Well preserved	Preserved	Preserved/mildly eroded	Well preserved	Absent (3D)	Low, dark blue-purple color	RAM-RAS	P2; P3; S1; IT3

Tab. 2 - Taphofacies (TAF-1 to 4) of the RAV tetrapod record based on mineralized tissue preservation.
*cancellous bone fluorescence **sectioned specimens.

Finally, post burial and diagenetic modifications of the RAV skeletal elements are mostly represented by strong lithostatic compression, in some cases resulting in the merging of distinct elements in a single surface (MPPPL 18797, V7101, V7102). Mineralogical alterations can be present in the form of silica impregnation and possible recrystallization (MPPPL 18797, MCLSC T1). Abrasion is rarely reported, most likely linked to recent weathering.

Within the frame of these reported preservational differences in a common taphonomic context, we propose four different taphofacies (see Table 2) based on modes of preservation of vertebrate hard tissues in the RAV. These taphofacies (listed as TAF-1 to TAF-4) are specimen-based rather than characteristic of specific stratigraphic levels (e.g., Boessnecker et al. 2014), and some overlap between the three RAV members. Major discriminating characters between taphofacies are the preservation of enamel (absent in TAF-1), compact bone (severely eroded in TAF-3, well preserved in TAF-4) and of the trabecular structure in the cancellous bone (collapsed in TAF-3).

Preferential occurrence of large adults

There is a remarkable body size consistency among the most complete deadfall specimens, with all likely representing adult or near-adult individuals between 3–5 m total length and with estimated carcass masses of >300 kg. There are some ecological and some taphonomic explanations for such homogeneity. Carcass persistence on the seafloor is related to scavenging rate, and therefore to carcass mass (Higgs et al. 2014). This is also expected to be true in the RAV, where smaller carcasses were likely more rapidly stripped of soft tissues (or consumed as a whole), thus resulting in longer exposure time intervals during which the bones and teeth were subjected to chemical dissolution and biological ero-

sion, and therefore resulting in decreased chances of fossilization. Likewise, the weakly mineralized, relatively more porous bone of ontogenetically young individuals (e.g., Houssaye et al. 2018) is expected to degrade more quickly than the more heavily mineralized bones of adults. This might explain why some small, relatively delicate bones persist in the preserved carcasses, but small individuals are entirely absent from the fauna. In tentative support of this, the smallest element of the vertebrate fauna (Aeolodontini indet., Table 1) whose estimated total length is only 1.5 m, is preserved as a regurgitalite, a preservation style thought to protect the skeleton from environmental degradation (Serafini et al. 2022). That said, the RAV also represents a pelagic offshore paleoenvironment, and as such it was likely frequented by adult individuals of larger species, with neonatal and small juvenile individuals possibly occupying shallower habitats closer to the paleo-coastline. A similar habitat partitioning between adults and juveniles can be observed in modern cetaceans (e.g., in *Balaenoptera acutorostrata* Lacépède, 1804; Robinson et al. 2023). As such, the biased fossil composition might be also partially related to ecology.

Deadfall ecology

Three of the four ecological stages described in modern whale-fall communities were cumulatively observed in RAV marine amniotes (Figs. 10, 11), based on either direct or indirect evidence. Interestingly, despite the small sample size, some components of the deadfall communities appear exclusive of some taxonomic groups. Cephalopods seem to be non-selective, exploiting carcasses of all three major groups of marine reptiles. Echinoid elements are instead only associated with the pliosaurid carcasses. Likewise, shark teeth are entirely absent from thalattosuchian deadfalls, but are present on both the pliosaurs and one of the two ichthy-

osaurs. Of the three groups, thalattosuchians have the lowest mass per unit length (i.e., a more slender body profile, and a greater surface area to volume ratio). This more elongated body might result in a more dispersed carcass-fall community, resulting in a decreased rate of detection for a given area of rock. Moreover, whereas ichthyosaurs and plesiosaurs likely had an endothermic thermophysiology, metriorhynchids maintained a cooler body temperature (Séon et al. 2020) and possibly lacked a thick blubber layer. Thus, as well as containing less mass per unit length, metriorhynchoid carcasses may also have represented less nutrient-rich habitats and attracted a less diverse exploiting fauna. Associated fauna is found in most of the RAV carcasses, with some taxa being more abundant and common than others (Fig. 11A–D).

Mobile scavenger stage – Shark teeth are confidently assigned to the mobile scavenger stage (Smith & Baco 2003; Smith 2015), with their occurrence being verified for three marine reptile oryctocoenoses (PLS T1; MPPPL 18797; V7101) and possible bite marks on MGP-PD 6761 (Fig. 10E). Elasmobranch teeth are not common in the RAV (Serafini et al. 2020), and with the exception of *Strophodus* (once commonly reported as *Asteracanthus*) and dubious lamniform teeth (Sirna et al. 1994), hexanchiforms comprise the majority of the finds (D'Erasmo 1922; Sirna et al. 1994). The close association of such rare finds with marine reptile remains can be parsimoniously attributed to scavenging activity rather than coincidental occurrence. Besides scavenging, active predation by hexanchiform sharks should not be completely ruled out, as modern Hexanchidae are also recognized as occasional predators of marine mammals (Heithaus, 2001). Among Hexanchiformes, here we report the presence of Hexanchidae as a component of the reptile-falls (Fig. 11E). Orthacodontidae (*Sphenodus*) either included in Hexanchiformes (Cappetta 2012) or in Synechodontiformes (Klug 2010), is also reported with a single tooth. Hexanchiforms are renowned for their ecological role as scavengers, both in Cenozoic-Recent forms (e.g., Hexanchidae; McNiels et al. 2016; Merella et al. 2021; 2022) and Mesozoic taxa (Bogan et al. 2016; Paparella et al. 2017; Serafini et al. 2020). Previous reports of hexanchiforms scavenging marine reptile carcasses allow this association to be traced back to the Upper Cretaceous (Bogan et al. 2016) and the Upper Ju-

rassic (Kimmeridgian; Paparella et al. 2017; Serafini et al. 2020). Our survey extends the record of this ecological role for the group earlier in time, with its occurrence at least from the middle Oxfordian and possibly from the upper Bajocian. Furthermore, evidence for a trophic interaction between hexanchiform sharks and a pliosaur carcass is also reported herein for the first time.

The second category of mobile scavengers that we recognize in the RAV tetrapod record are cephalopods (Fig. 11A, E). Rhyncholites (s.l.) are isolated calcified pointed elements from the upper jaw (tip of the upper beak) of nautiloids and some ammonoids (Nixon 1988; Riegraf & Moosleitner 2010; Mironenko et al. 2021). Isolated mouth parts of cephalopods are problematic: among different types of buccal-jaw apparatuses that can be found in fossil cephalopods (Tanabe et al. 2015), calcitic parts historically followed their own parataxonomy, rarely with direct correspondence to *in situ* preserved elements (Riegraf & Moosleitner 2010). Calcified jaw tips (rhyncholites and conchorhyncs, respectively upper and lower jaw tip) were historically attributed exclusively to nautiloids (McFarlan & Campbell 1991) but some ammonoids were, more recently, also recognized as possessing such structures (Phylloceratina, Lytoceratina; Tanabe et al. 2015). The best-known calcified beak-bearing ammonoids are from the Upper Cretaceous (e.g., *Hypophylloceras*, *Phyllopachyceras, Tetragonites;* Tanabe et al. 2015), but the presence of a possible thin calcareous layer over the lower jaw of a Middle Jurassic Phylloceratina was also reported by Mironenko & Gulyaev (2018). Rhyncholites are well known from the RAV (Dieni 1975; Martire 1996) and were historically attributed to the paragenera *Gonatocheilus* and *Leptocheilus* (Laub 1994). Interestingly, rhyncholites are more common than nautiloid internal molds in the RAV (Laub 1994; Fig. 11F) and it is possible that the calcified tips of the beak were shed during feeding. All the jaw elements that we identified from RAV vertebrate carcasses are here listed as rhyncholites, but for the smaller specimens (fragmentary tips) we cannot exclude the presence also of some conchorhyncs. Due to their poor preservation, we cannot confidently assign these rhyncholites to any paragenus; however, they more closely resemble the nautiloid morphotypes (arrowhead shape, also found in the modern *Nautilus*; Nixon 1988; Klug 2001) rather than the Cretaceous ammonoid mor-
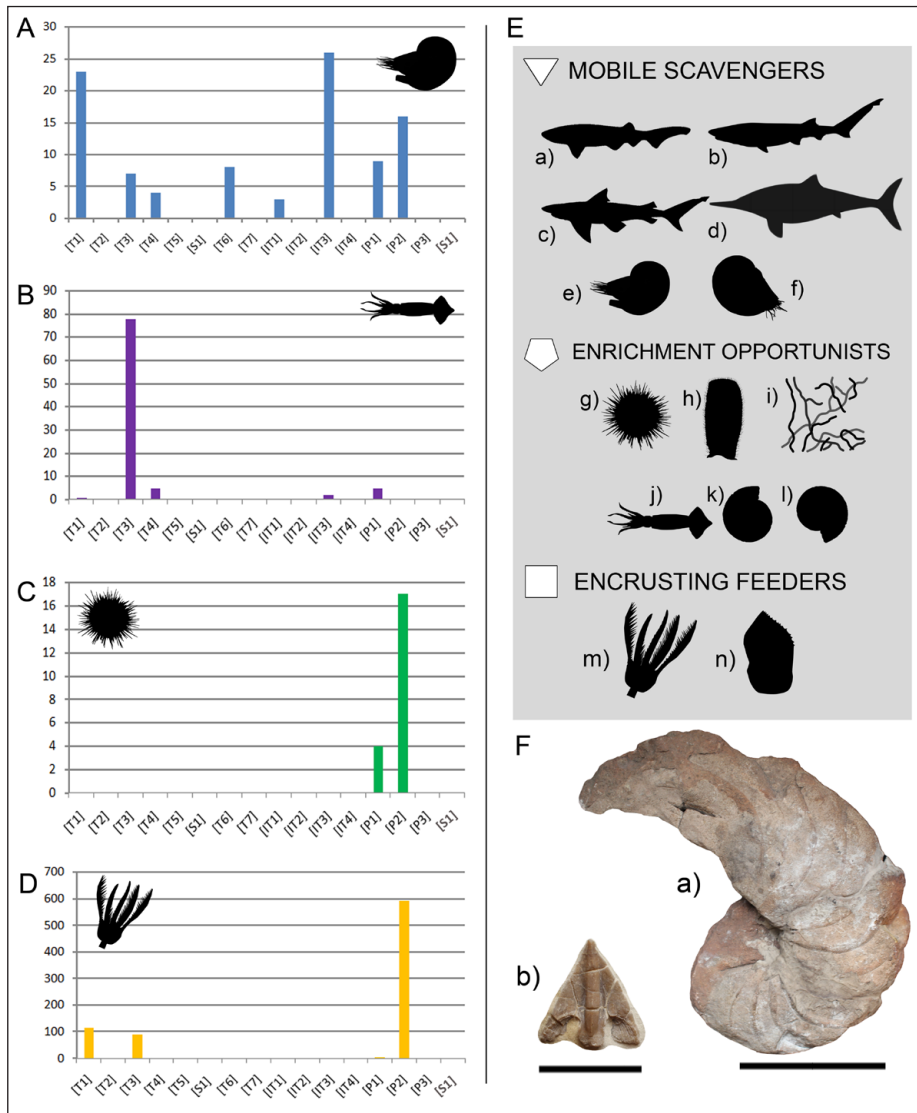
Fig. 11 - Summary of the principal faunal associations from the RAV marine reptile falls. A) Abundance histogram for rhyncholites. B) Abundance histogram for belemnites. C) Abundance histogram for echinoids. D) Abundance histogram for crinoid elements. Bracketed labels on the x axes correspond to those of Table 1. E) Summary of the retrieved deadfall stages. Silhouettes: a) *Notidanodon* sp. modified after *Hexanchus griseus* by Marc Dando in Ebert *et al.* 2015; b) cf. *Pseudonotidanus* from *Notorynchus cepedianus* by Ignacio Contreras (CC BY 3.0 Deed); c) *Sphenodus* sp. modified after Böttcher and Duffin 2000; d) Ichthyosauria (modified after Sissons *et al.* 2015); e) Nautiloid (*Gonatocheilus*-like bearing rhyncholite) CC0 1.0 by Dean Schnabel; f) Nautiloid (*Leptocheilus*-like bearing rhyncholite) CC0 1.0 by Margot Michaud; g) Echinoidea CC0 1.0 by Christoph Schomburg; h) Porifera CC0 1.0 by Guillaume Dera; i) Endolithic fungi by Matt Crook (CC BY-SA 3.0 Deed); j) *Hibolites* from *Illex illecebrosus* CC0 1.0 by Nathan Hermann; k) Ammonoid (*Laevaptychus*-bearing aptychus) CC0 1.0 by Margot Michaud; l) Ammonoid (*Lamellaptychus*-bearing aptychus) modified from k); m) Phyllocrinid crinoid CC0.1.0 by Lauren Sumner-Rooney; n) Pholadid bivalve as the producer of *Gastrochaenolites* CC0 1.0 by Katie Collins. F) a) Rare Middle Jurassic nautiloid internal mold (MGP-PD 32650) from the RAI and b) Upper Jurassic isolated rhyncholite (MGP-PD 20436). Scale bar Fa) 5 cm; Fb) 2 cm.

photype (Tanabe et al. 2015; C. Klug pers. comm. 2023; G. Schweigert pers. comm. 2023). We cannot completely exclude the possibility that some of the surveyed cephalopod beak tips might belong to ammonoids, but since the only confirmed, highly calcified ammonoid jaws are known *in situ* from the Upper Cretaceous, we find it safe to assume these are most likely from nautiloids. Here we present strong evidence that these nautiloid jaw elements are linked to scavenging of RAV marine reptile carcasses from the upper Bajocian to the Kimmeridgian. Beside the high numbers of rhyncholites that occur near the surveyed specimens, we also provide evidence of beak tips piercing the bone in two separate cases (PBS of MCLSC T1 and frontal of PLS T1; Figs. 3D, 8B), which suggests active exploitation of the carcasses. Although already speculated from traces on bones (Maxwell et al. 2022), to our knowledge this is the first reported occurrence of direct active

scavenging by nautiloids on Mesozoic marine reptiles, including thalattosuchians, pliosaurs and ophthalmosaurian ichthyosaurs. Extant nautiloids are known to scavenge fish carcasses (e.g., Dunstand et al. 2011), where upper and lower beaks are used to scrape the meat, aided by labial tentacles (Sasaki et al. 2010). Rhyncholites are by far more represented than shark teeth in RAV reptile-falls (Fig. 11A), possibly suggesting a common and predominant occurrence of nautiloids as scavengers in Middle-Upper Jurassic deep-water settings.

The last representative of the mobile scavenger stage that we recognized is a single ichthyosaur tooth found stuck on a rib of V7101 (unlikely to represent predation based on crown size and shape, discussed in detail in Serafini et al. (2020)), suggesting that other marine reptiles also took advantage of necrophagy, possibly when the carcasses were floating.

Enrichment-opportunist stage – Opportunistic exploiters of the surveyed RAV carcasses are more difficult to frame. We are confident in assigning echinoids to the enrichment-opportunist stage (Smith & Baco 2003; Smith 2015). Echinoids are rare from RAV deposits, so finding them in relatively large numbers associated with a carcass (Fig. 11C) is a strong indication of their specific occurrence in nutrient-rich conditions. Known echinoids from the RAV are the irregular taxa *Cyclolampas* and *Cardiolampas* (Sarti 1993), but we cannot advance any reliable attribution of our material (outside being regular echinoids, possibly cidaroids) due to incompleteness. Previously reported RAV echinoids are bathyal taxa (Sarti 1993); therefore, their presence is still consistent with a deep-water paleoecological interpretation of the deposit. Echinoids were attributed to the enrichment opportunist stage in an Upper Jurassic deadfall by Danise et al. (2014), where distinctive traces of their grazing activity (possibly for foraging microbial mats) were recognized on the bones. Similarly, Maxwell et al. (2022) attributed to the same stage echinoids from Lower Jurassic Posidonia Shale carcasses. It is likely that the echinoid elements that we report here belonged to similarly opportunistic grazers of the skeletonized carcasses; the presence of superficial bioerosion in the compact bone of a RAV ichthyosaur rostrum (V7158; Serafini et al. 2023a; Fig. 10F) might support this grazing exploitation hypothesis, although other invertebrate producers (e.g., sponges) cannot be ruled out.

In the context of bioerosion, the unbranched and millimetric borings found in the maxilla and teeth of MM 25.5.1078 (Serafini et al. 2023b; Fig. 10C, D) can be confidently assigned to the enrichment-opportunist stage (Fig. 11E). Producers of similar traces are clionid sponges (Wisshak et al. 2019; Jamison-Todd et al. 2023) and (only by shape but inconsistently with sizes) endolithic marine fungi (Martill 1989; Golubic et al. 2005). Borings appear to penetrate the compact and cancellous bone in a straight line (Fig. 10C), while when they affect teeth they penetrate the dentine in a circle, contouring the pulpal cavity. Such a deep and localized penetration appears to be indicative of active nutrient exploitation rather than alteration during encrustation of the bones. A similar exploitation can be traced microscopically on the trabeculae of MPPPL 18797, V7101 and MCLSC T1, with bacterial and fungal microborings (Fig. 10A, B; see also Danise et al. 2012).

The last association that could be linked to the opportunist stage are belemnite rostra and ammonite aptychi. Both cephalopod elements are common in the RAV, so their presence needs to be carefully discriminated from coincidental occurrence. We do not have strong evidence that ammonite aptychi are related to the deadfall ecology, since they could just represent the preserved parts of ammonites (the aragonite shell dissolves while calcitic parts remain). However, they could also be indicative of the presence of ammonoids attracted by the enriched environment around the carcass, possibly for foraging on other smaller invertebrates. Belemnites (*Hibolites*) could be considered coincidental, if not for the case of the *N. ammoniticus* holotype (Figs. 4B, 10B): the high abundance of belemnites associated with MGGC 8846/1UCC123a (and the other holotypic slabs) is unusual for their close proximity to the skull (sometimes with individuals set between cranial bones) and for the absence of a preferential orientation of the rostra. High density of belemnites in RAV hardgrounds is typical of condensed layers, but in such conditions the rostra follow the same orientation, usually parallel to the stratum polarity (Sarti 1993; Martire 1996). Mass deaths of belemnites (belemnite "battlefields") are speculated to be either the result of catastrophic events (e.g., sudden anoxia, volcanic eruptions), gut contents of teutophagic predators or related to the mass mortality after spawning typical of coleoids (Doyle & McDonald 1993). This last scenario is perhaps the more plausible for the *N. ammoniticus* specimen, where a large group of *Hibolites* might have gathered for mating in the surroundings of the nutrient-rich metriorhynchid deadfall. In modern schooling squids (e.g., *Doryteuthis opalescens* (Berry, 1911)) the reproductive effort results in the death of the adults (Fields 1965; Perretti et al. 2016), which sink from a few hours after spawning and up to 11 days after mating to the seafloor without a preferential orientation (Doyle & McDonald 1993). Perretti et al. (2016) describeshow some adults cease movement and die in a few hours after spawning, while some males engage in egg-guarding behavior, which both justify the large occurrence of dead adults in the same surroundings as the spawning ground. The presence of a post-spawning mass mortality in the proximity of a deadfall is likely not coincidental. Adults might have exploited trophic resources from the carcass, but we also believe it is plausible that the deadfall enriched

surroundings might have been selected as a resource for the hatchling paralarvae (Perretti, pers. comm, 2024) as modern *D. opalescens* adults stop feeding right before and after mating (Perretti et al. 2016). This is, however, speculative and needs further research. While impossible to assess for all *Hibolites* preserved in the slab due to differently oriented cuts, many specimens are consistent in size, which would seemingly support the preferential occurrence of sexually mature individuals. We assign this possible deadfall-exploitation during mating gathering to the enrichment opportunistic stage; this attribution consequently makes belemnites from other RAV deadfalls possible opportunists of pelagic reptile carcasses.

Sulfophilic stage – The sulfophilic stage was not detected in the RAV sample (File S1). Mesozoic taxa known for hosting chemosynthetic sulfur-reducing bacterial symbionts (e.g., lucinid or solemyid bivalves; Jenkins et al. 2013) were not identified in association with the surveyed carcasses. Similarly, pyrite framboids, a proxy for sulfur microbial mobilization during lipid decay, were not found inside the bone spongiosa of MPPPL 18797, V7101 and MCLSC T1. We believe that the lack of evidence for this stage could be environmental, as pyrite framboids, which were found in bones of both shallower (Danise et al. 2014) and deeper (Serafini et al. 2023c) settings might not had formed (or preserved) due to the constant oxic conditions at the RAV seafloor.

Reef stage – Suspension feeders that can be assigned to the reef stage are crinoids and possibly boring bivalves (Figs. 10G, 11E). Crinoid elements (most likely from Phyllocrinidae) are widespread between the cancellous bone of many RAV specimens (Fig. 11D). Such severe colonization of bare bones by crinoids has not been reported in previous deadfall studies (Fujiwara et al. 2007; Dick 2015; Maxwell et al. 2022). Dick (2015) reported the presence of crinoid elements in the surroundings of ichthyosaur carcasses from the Posidonia Shale, which were later considered rare by Maxwell et al. (2022). It is likely that encrusting crinoids growing on bones could be exclusive, or usually limited, to deep-water settings, such as the RAV. The only scenario that we can feasibly hypothesize for the occurrence of crinoid stem articula deeply embedded within cancellous bone (Fig. 10G), is that the crinoid planktonic larvae might have landed on an already deeply eroded unburied skeleton on the seafloor and grown into the sessile adult form, erupting from the trabecular

structure. Modern crinoid larval stages (auricolaria-like and doliolaria) are about 700 μm long and 400 μm wide (Nakano et al. 2003), therefore capable of fitting in intratrabecular spaces.

Gastrochaenolites-like clavate erosion can be found on the mandibular ramus of MCLSC T1 (Fig. 8G, H); these traces could be produced by boring bivalves (e.g., Pholadidae), common reef-stage components of vertebrate deadfalls (Belaústegui et al. 2012; Amalfitano et al. 2019; Maxwell et al. 2022). The only physical bivalve that could be found on a RAV carcass (Bivalvia indet. on MPPPL 18797; Fig. 6G) might be interpreted as a possible encrusting suspension feeder.

Differences with shallow-water deadfall communities

RAV deadfall communities are different from previously described reptile carcass-associated faunas (Danise et al. 2014; Dick 2015; Maxwell et al. 2022), with faunal association poorer in both taxonomic composition and individual abundance. This low diversity can be explained by the strong preservational bias characteristic of the RAV deposit, with dissolution phenomena also affecting the associated fauna. However, it is also possible that the RAV record is indicative for an environmentally driven lower diversity of carbonate contributors to the deadfall community compared to shallower settings. The reef stage is usually better and more commonly represented in epicontinental deposits (Danise et al. 2014; Maxwell et al. 2022), with a distinctive contribution of bivalves (mostly ostreids) and serpulid polychaetes in the encrustation of skeletal elements. In RAV deadfalls, crinoids appear to occupy the reef stage niche, possibly outcompeting other encrusting suspension feeders. Ophiuroids, a common deadfall opportunist (Maxwell et al 2022), were not found in the proximity of RAV carcasses; this absence most likely reflects a preservational effect rather than an ecological difference between shallow and deep-water deadfall communities since, in modern oceans, ophiuroids are also found associated with whale falls from outer shelf and bathyal settings (Bennet et al. 1994; Fujiwara et al. 2007). RAV mobile scavengers also deviate from Mesozoic fossil deadfalls: hexanchiforms are usually not reported in shallow-water deadfalls, which instead appear to have been more often exploited by hybodont sharks during the Middle Jurassic (Martill

1991). The abundance of hybodonts had declined in open marine assemblages by the Late Jurassic (Rees & Underwood 2008), which may have made deep-water scavenging niches available for the neoselachian hexanchiforms. Lamniforms and carcharhinids dominate the early scavenger niche in extant (Clua et al. 2013) and fossil (e.g., Bosio et al. 2021) coastal settings, with multiple reports also in the Mesozoic (e.g., in the Upper Cretaceous of the Western Interior Seaway: Schwimmer et al. 1997; Konishi et al. 2014). In contrast, hexanchids are common scavengers in Recent deep-water settings (McNiels et al. 2016), with only juveniles inhabiting shallow coastal waters, most likely to avoid intraspecific competition and cannibalistic predation (Rodríguez-Cabello et al. 2018). Exceptions to this deep-water segregation have been reported for hexanchiforms (Merella et al. 2021; Bisconti et al. 2023), but only in Cenozoic marine mammal-falls. Cephalopods have not previously been described as playing such a predominant role in Mesozoic mobile scavenger stages such as in RAV deadfalls: we believe that this might also represent a shallow-water bias, since modern cephalopods are known to exploit whale carcasses in bathyal zones in large numbers (e.g., *Mussoctopus* in Monterey Bay on a baleen whale; Nautilus live.org). Moreover, the presence of nautiloids is also strongly indicative of a deep-water environment, as the group is known to inhabit maximum depths between 200 and 800 m depending on the species, based on estimates of shell implosion limits (e.g., Dunstand et al. 2011; Hoffmann et al. 2019). Future studies on the paleobathymetry of the RAV might also consider extrapolating depth information from nautiloids, if diagnostic specimens are retrieved. Thanks to the vertebrate taphonomic data and deadfall composition, we provide new evidence in favor of a bathyal, deep-water interpretation of the RAV depositional setting as previously proposed elsewhere (e.g., Winterer 1998).

Conclusions

With the present study, we provide the first inclusive taphonomic revision of the marine tetrapod record from the Middle-Upper Jurassic of the Rosso Ammonitico Veronese (RAV). Our survey revealed:

A common poor state of preservation consistent with the prolonged exposure of carcasses on a well-oxygenated seafloor. This aspect is particularly evident in the erosion of compact bone in almost every specimen.

Evidence of chemical dissolution of hard tissues, unexpectedly also of enamel exposed at the water-sediment interface.

Different specimen-based taphofacies based on the mode of preservation of vertebrate hard tissues (enamel, dentine, acellular cementum, compact bone, cancellous bone).

Moreover, based on the analysis of the associated fossil fauna, we were able to identify deadfall stages analogous to modern whale-falls. Our results show:

A mobile scavenger stage witnessed by hexanchiform sharks (*Notidanodon* sp., cf. *Pseudonotidanus* sp., and *Sphenodus* sp.), nautiloid beak elements and rare teeth of marine reptiles. For the first time we unambiguously document the active trophic interaction of Mesozoic nautiloids with marine reptile carcassess during scavenging.

An enrichment opportunist stage that features deep-water echinoids, bioeroders compatible with sponges or marine fungi, possibly ammonoid aptychi, and occasionally large occurrences of belemnites (cf. *Hibolites*) believed to have died in large numbers after a spawning congregation in the surroundings of an organic-enriched carcass.

A reef stage almost exclusively dominated by crinoids (cf. Phyllocrinidae) as suspension feeders encrusting the skeletal elements. We hypothesize that the planktonic larvae could have landed in the cancellous bone already exposed by chemical erosion and then grown into the adult sessile form deeply embedded inside the bone itself. We report this peculiar encrustation with large numbers of individuals affecting tetrapod bones for the first time. Clavate erosions similar to *Gastrochaenolites* are also interpreted as reef-stage suspension feeders similar to modern pholadid bivalves.

While some of our results deviate from other Mesozoic deadfalls set in shallow waters, they are consistent with Recent whale-falls in pelagic-bathyal zones. These data support a bathyal interpretation of the RAV paleoenvironment. Our survey systematically characterized the taphonomy and deadfall ecology of a pelagic deposit from the Mesozoic, an environment often neglected due to the paucity

of specimens and their poor preservation. Future studies on similar or deeper environments can further help us to better frame the evolution of deadfall-specialist clades in deep time, together with a better understanding of the ecological role of large pelagic reptiles in the Mesozoic oceans, during and after their lives.

REFERENCES

Allison P.A., Smith C.R., Kukert H., Deming J.W. & Bennett B.A. (1991) - Deep-water taphonomy of vertebrate carcasses. a whale skeleton in the bathyal Santa Catalina Basin. *Paleobiology*, 17: 78–89.

Amalfitano J., Giusberti L., Fornaciari E., Dalla Vecchia F.M., Luciani V., Kriwet J. & Carnevale G. (2019) - Large deadfalls of the "ginsu" shark *Cretoxyrhina mantelli* (Agassiz, 1835) (Neoselachii, Lamniformes) from the Upper Cretaceous of northeastern Italy. *Cretaceous Research*, 98: 250–275.

Barbieri G. & Ginevra M. (1995) - L'attività estrattiva di marmi nell'Altopiano dei Sette Comuni. Passato e Presente (Prealpi Venete). *Studi Trentini di Scienze Naturali, Acta Geologica*, 70: 165–179.

Beardmore S.R. & Furrer H. (2016) - Evidence of a preservational gradient in the skeletal taphonomy of Ichthyopterygia (Reptilia) from Europe. *Palaeogeography, Palaeoclimatology, Palaeoecology*, 443: 131–144.

Beardmore S.R., Orr P.J., Manzocchi T. & Furrer H. (2012) - Float or sink: modelling the taphonomy pathway of marine crocodiles (Mesoeucrocodylia; Thalattosuchia) during the death-burial interval. In: Wuttke, M., Reisdorf, A.G. (Eds.), Special Issue: Taphonomic Processes in Terrestrial and Marine Environments. *Palaeobiodiversity and Palaeoenvironment*, 92: 83–98.

Belaústegui Z., De Gibert J.M., Domnèch R., Muñiz F. & Martinell J. (2012) - Clavate borings in a Miocene cetacean skeleton from Tarragona (NE Spain) and the fossil record of marine bone bioerosion. *Palaeogeography, Palaeoclimatology, Palaeoecology*, 323-325: 68–74.

Bennet B.A., Smith C.R., Glaser B. & Maybaum H.L. (1994) - Faunal community structure of a chemoautotrophic assemblage on whale bones in the deep northeast Pacific Ocean. *Marine Ecology Progress Series*, 108: 205–223.

Bisconti M., Chicchi S., Monegatti P., Scacchetti M., Campanini M., Marsili S. & Carnevale G. (2023) - Taphonomy, osteology and functional morphology of a partially articulated skeleton of an archaic Pliocene right whale from Emilia Romagna (NW Italy). *Bollettino della Società Paleontologica Italiana*, 62: 1–22.

Bizzarini F. (1996) - Sui resti di coccodrillo del Rosso Ammonitico veronese di Sasso di Asiago (Altopiano dei Sette Comuni, Prealpi Venete). *Annali del Museo Civico di Rovereto*, 11: 339–348.

Bizzarini F. (2003) - L'ittiosauro del Museo Civico della Laguna Sud. Chioggia. *Rivista di Studi e Ricerche, Chioggia*, 23: 117–124.

Boessenecker R.W., Perry F.A. & Schmitt J.G. (2014) - Comparative Taphonomy, Taphofacies, and Bonebeds of the Mio-Pliocene Purisima Formation, Central California: Strong Physical Control on Marine Vertebrate Preservation in Shallow Marine Settings. *PLoS ONE*, 9(3): e91419.

Bogan S., Agnolin F. & Novas F. (2016) - New selachian records from the Upper Cretaceous of southern Patagonia: paleobiogeographical implications and the description of a new taxon. *Journal of Vertebrate Paleontology*: e1105235.

Bosellini A., Masetti D. & Sarti M. (1981) - A Jurassic "Tongue of the ocean" infilled with oolitic sands: the Belluno

Trough, Venetian Alps, Italy. *Marine Geology*, 44(1-2): 59–95.

Bosio G., Collareta A., Di Celma C., Lambert O., Marx F.G., De Muizon C., Gioncada A., Gariboldi K., Malinverno E., Malca R.V., Urbina M. & Bianucci G. (2021) - Taphonomy of marine vertebrates of the Pisco Formation (Miocene, Peru): Insights into the origin of an outstanding Fossil-Lagerstätte. *PLoS ONE*, 16(7): e0254395.

Böttcher R. & Duffin C. (2000) - The neoselachian shark *Sphenodus* from the Late Kimmeridgian (Late Jurassic) of Nusplingen and Egesheim (Baden-Württemberg, Germany). *Stuttgarter Beitrage zur Naturkunde, Serie B*, 283: 1–31.

Bown P.R. & Young J.R. (1998) - Techniques. In: Bown PR. (Ed) - Calcareous nannofossil biostratigraphy. British Micropaleontological Society Publications Series: 16–28. Kluwer Academic Publishers, London.

Boyde A. (1971) - Comparative histology of mammalian teeth. In: Dahlberg A. (Ed) - Dental Morphology and Evolution: 81–94. Chicago University Press, Chicago.

Cappetta H. (2012) - Chondrichthyes (Mesozoic and Cenozoic Elasmobranchii: teeth). In: Schultze H.-P. (Ed) - Handbook of Paleoichthyology. 3E. Verlag Dr. Friedrich Pfeil, München, 512 pp.

Casellato C.E. (2010) - Calcareous nannofossil biostratigraphy of upper Callovian–lower Berriasian successions from the Southern Alps, North Italy. *Rivista Italiana di Paleontologia e Stratigrafia*, 116: 357–404.

Cau A. (2019) - A revision of the diagnosis and affinities of the metriorhynchoids (Crocodylomorpha, Thalattosuchia) from the Rosso Ammonitico Veronese Formation (Jurassic of Italy) using specimen-level analyses. *PeerJ*, 7: e7364.

Cau A. & Bizzarini F. (2020) - Preliminary report of a new pliosaurid specimen (Reptilia, Plesiosauria) from the Rosso Ammonitico Veronese Formation (Middle-Upper Jurassic of Italy). *Bollettino della Società Paleontologica Italiana*, 59: 175–177.

Cau A. & Fanti F. (2011) - The oldest known metriorhynchid crocodilian from the Middle Jurassic of North-eastern Italy: *Neptunidraco ammoniticus* gen. et sp. nov. *Gondwana Research*, 19: 550–565.

Cau A. & Fanti F. (2014) - A pliosaurid plesiosaurian from the Rosso Ammonitico Veronese Formation of Italy. *Acta Palaeontologica Polonica*, 59(3): 643–650.

Cau A. & Fanti F. (2016) - High evolutionary rates and the origin of the Rosso Ammonitico Veronese Formation (Middle–Upper Jurassic of Italy) reptiles. *Historical Biology*, 28: 952–962.

Clari P.A., Marini P., Pastorini M. & Pavia G. (1984) - Il Rosso Ammonitico Inferiore (Baiociano-Calloviano) nei Monti Lessini settentrionali (Verona). *Rivista Italiana di Paleontologia e Stratigrafia*, 90(1): 15–86.

Clari P.A., Martire L. & Pavia G. (1990) - L'unità selcifera del Rosso Ammonitico Veronese (Alpi Meridionali). In: Atti II Convegno Internazionale "Fossili, Evoluzione, Ambiente", Pergola II, 1987: 151-162. Ancona.

Cleary T.J., Moon B.C., Dunhill A.M. & Benton M.J. (2015) - The fossil record of ichthyosaurs, completeness metrics and sampling biases. *Palaeontology*, 58(3): 521–536.

Clua E., Chauvet C., Read T., Werry J. & Lee S. (2013) - Behavioural patterns of a Tiger Shark (*Galeocerdo cuvier*) feeding aggregation at a blue whale carcass in Prony Bay, New Caledonia. *Marine and Freshwater Behaviour and Physiology*,

46: 1–20.

Danise S., Cavallazzi B., Dominici S., Westall F., Monechi S. & Guioli S. (2012) - Evidence of microbial activity from a shallow water whale fall (Voghera, northern Italy). *Palaeogeography, Palaeoclimatology, Palaeoecology*, 317: 13–26.

Danise S., Twitchett R.J. & Matts K. (2014) - Ecological succession of a Jurassic shallow–water ichthyosaur fall. *Nature Communications*, 5: 4789.

Danise S. & Dominici S. (2014) - A record of fossil shallow-water whale falls from Italy. *Lethaia*, 47: 229–243.

De Buffrénil V., De Ricqlès A.J., Zylberberg L. & Padian K. (2021) - Vertebrate skeletal histology and paleohistology. CRC Press, Boca Raton and London, 838 pp.

Delsett L.L., Novis L., Roberts A.J., Koevoets M., Hammer O., Druckenmiller P.S. & Hurum H.J. (2016) - The Slottsmøya marine reptile Lagerstätte: Depositional environments, taphonomy and diagenesis. *Geological Society of London, Special Publications*, 434: 165–188.

Delsett L.L., Roberts A.J., Druckenmiller P.S. & Hurum J.H. (2019) - Osteology and phylogeny of Late Jurassic ichthyosaurs from the Slottsmøya Member Lagerstätte (Spitsbergen, Svalbard). *Acta Palaeontologica Polonica*, 64(4): 717-743

D'Erasmo G. (1922) - Catalogo dei pesci fossili delle Tre Venezie. *Memorie dell'Istituto Geologico della Regia Università di Padova*, 6: 1–181.

Dick D.G. (2015) - An ichthyosaur carcass-fall community from the Posidonia Shale (Toarcian) of Germany. *Palaios*, 30: 353–361.

Dieni I. (1975) - Revisione di alcune specie giurassiche e cretacee di rincoliti. *Palaeontographia Italica*, 69: 38–107.

Doyle P. & Macdonald D.I.M. (1993) - Belemnite battlefields. *Lethaia*, 26: 65–80.

Dunstan A.J., Ward P.D. & Marshall N.J. (2011) - Vertical Distribution and Migration Patterns of *Nautilus pompilius*. *PLoS ONE*, 6(2): e16311.

Ebert D., Dando M. & Bodiguel C. (2015) - On board guide for the identification of pelagic sharks and rays of the Western Indian Ocean. FAO/IOC, 120 pp.

Fields W.G. (1965) - The structure, development, food relations, reproduc-tion and life history of the squid *Loligo opalescens* Berry. California Department of Fish and Game. *Fish Bulletin*, 131: 1–108.

Flores J.A. & Sierro F.J. (1997) - Revised technique for calculation of calcareous nannofossil accumulation rates. *Micropaleontology*, 43: 321–324.

Flügel E. (2010) - Microfacies of carbonate rocks: analysis, interpretation and application. Munnecke, Axel. (2nd ed.). Heidelberg: Springer, 976 pp.

Foffa D., Cuff A.R., Sassoon J., Rayfield E.J., Mavrogordato M.N. & Benton M.J. (2014) - Functional anatomy and feeding biomechanics of a giant Upper Jurassic pliosaur (Reptilia: Sauropterygia) from Weymouth Bay, Dorset, UK. *Journal of Anatomy*, 225(2): 209–219.

Fujiwara Y., Kawato M., Yamamoto T., Yamanaka T., Sato-Okoshi W., Noda C., Tsuchida S., Komai T., Cubelio S.S., Sasaki T., Jacobsen K., Kubokawa K., Fujikura K., Maruyama T., Furushima Y., Okoshi K., Miyake H., Miyazaki M., Nogi Y., Yatabe A. & Okutani T. (2007) - Three-year investigations into sperm whale-fall ecosystems in Japan. *Marine Ecology*, 28: 219–232.

Georgieva M.N., Wiklund H., Ramos D.A., Neal L., Glasby C.J. & Gunton L.M. (2023) - The annelid community of a natural deep-sea whale fall off eastern Australia.

Records of the Australian Museum, 75(3): 167–213.

Glover A.G., Källström B., Smith C.R. & Dahlgren T.G. (2005) - World–wide whale worms? A new species of *Osedax* from the shallow north Atlantic. *Proceedings of the Royal Society B*, 272: 2587–2592.

Goffredi S.K. & Orphan V.J. (2010) - Bacterial community shifts in taxa and diversity in response to localized organic loading in the deep sea. *Environmental Microbiology*, 12: 344–363.

Goffredi S.K., Wilpiszeski R., Lee R. & Orphan V. (2008) - Temporal evolution of methane cycling and phylogenetic diversity of archaea in sediments from a deep-sea whale-fall in Monterey Canyon, California. *ISME Journal*, 2: 204–220.

Golubic S., Radtke G. & Le Campion-Alsumard T. (2005) - Endolithic fungi in marine ecosystems. *Trends in Microbiology*, 13: 229–235.

Gutarra S., Moon B.C., Rahman I.A., Palmer C., Lautenschlager S., Brimacombe A.J. & Benton M.J. (2019) - Effects of body plan evolution on the hydrodynamic drag and energy requirements of swimming in ichthyosaurs. *Proceedings of the Royal Society B*, 286: 20182786.

Gutarra S., Stubbs T.L., Moon B.C., Palmer C. & Benton M.J. (2022) - Large size in aquatic tetrapods compensates for high drag caused by extreme body proportions. *Communications Biology*, 5(1): 380.

Gutarra S. & Rahman I.A. (2021) - The locomotion of extinct secondarily aquatic tetrapods. *Biological Reviews*, 97: 67–98.

Hedges R.E.M. (2002) - Bone diagenesis: an overview of processes. *Archaeometry*, 44: 319–328.

Hess H. (2012) - Crinoids from the Middle Jurassic (Bajocian–Lower Callovian) of Ardèche, France. *Swiss Journal of Palaeontology*, 131: 211–253.

Hoffmann R., Riechelmann S., Ritterbush K.A., Koelen J., Lübke N., Joachimski M.M., Lehmann J. & Immenhauser A. (2019) - A novel multiproxy approach to reconstruct the paleoecology of extinct cephalopods. *Gondwana Research*, 67: 64–81.

Heithaus M.R. (2001) - Predator–prey and competitive interactions between sharks (order Selachii) and dolphins (suborder Odontoceti): a review. *Journal of Zoology*, 253(1): 53-68.

Higgs N.D., Gates A.R. & Jones D.O.B. (2014) - Fish food in the deep sea: revisiting the role of large food-falls. *PLoS ONE*, 9: e96016.

Hogler J.A. (1994) - Speculations on the role of marine reptile deadfalls in Mesozoic deep-sea paleoecology. *Palaios*, 9: 42–47.

Houssaye A., Scheyer T.M., Kolb C., Fischer V. & Sander P.M. (2014) - A new look at ichthyosaur long bone microanatomy and histology: implications for their adaptation to an aquatic life. *PLoS ONE*, 9: e95637.

Houssaye A., Nakajima Y. & Sander P.M. (2018) - Structural, functional, and physiological signals in ichthyosaur vertebral centrum microanatomy and histology. *Geodiversitas*, 40: 161–170.

Jacobs M.L. & Martill D.M. (2020) - A new ophthalmosaurid ichthyosaur from the Upper Jurassic (Early Tithonian) Kimmeridge Clay of Dorset, UK, with implications for Late Jurassic ichthyosaur diversity. *PLoS ONE*, 15(12): e0241700.

Jamison-Todd S., Upchurch P. & Mannion P. (2023) - The prevalence of invertebrate bioerosion on Mesozoic marine reptile bone from the Jurassic and Cretaceous of the United Kingdom: New data and implications for taphonomy and environment. *Geological Magazine*, 160(9): 1701–1710.

Jenkins R.G., Kaim A., Little C.T.S., Iba Y., Tanabe K. & Campbell K.A. (2013) - Worldwide distribution of the modiomorphid bivalve genus *Caspiconcha* in late Mesozoic hydrocarbon seeps. *Acta Palaeontologica Polonica*, 58 (2): 357–382.

Kaim A., Kobayashi Y., Echizenya H., Jenkins R.G. & Tanabe K. (2008) - Chemosynthesis-based associations on Cretaceous plesiosaurid carcasses. *Acta Palaeontologica Polonica*, 53: 97–104.

Kendall C., Eriksen A.M.H., Kontopoulos I., Collins M.J. & Turner-Walker G. (2018) - Diagenesis of archaeological bone and tooth. *Palaeogeography, Palaeoclimatology, Palaeoecology*, 491: 21–37.

Klug C. (2001) - Functional morphology and taphonomy of nautiloid beaks from the Middle Triassic of southern Germany. *Acta Palaeontologica Polonica*, 46: 43–68.

Klug S. (2010) - Monophyly, phylogeny and systematic position of the †Synechodontiformes (Chondrichthyes, Neoselachii). *Zoologica Scripta*, 39: 37–49.

Konishi T., Newbrey M.G.& Caldwell M.W. (2014) - A small, exquisitely preserved specimen of *Mosasaurus missouriensis* (Squamata, Mosasauridae) from the upper Campanian of the Bearpaw Formation, western Canada, and the first stomach contents for the genus. *Journal of Vertebrate Paleontology*, 34(4): 802–819.

Laub C. (1994) - The Radiolarit-Rhyncholithen-Kalke of the Rosso Ammonitico in the Central Southern Alps (Middle/Upper Jurassic, North Italy). *Palaeontographica*, A, 234: 89–166.

Macfarlan D.A.B. & Campbell J.D. (1991) - Rhyncholites (cephalopod mandibles) from the Late Triassic (Norian) of New Zealand and New Caledonia. *Journal of the Royal Society of New Zealand*, 21(2): 161–168.

Martill D.M. (1985) - The preservation of marine vertebrates in the Lower Oxford Clay (Jurassic) of central England. *Philosophical Transactions of the Royal Society of London*. B, 311: 155–165.

Martill D.M. (1989) - Fungal borings in neoselachian teeth from the lower Oxford Clay of Peterborough. *Mercian Geologist*, 12: 1–5.

Martill D.M., Cruickshank A.R.I. & Taylor M.A. (1991) - Dispersal via whale bones. *Nature*, 351: 193.

Martill D.M. (1991) - Marine Reptiles. In: Martill D.M. & Hudson J.D. (Eds) - Fossils of the Oxford Clay, Palaeontological Association Field Guide to Fossils, 4: 226–243. London, UK: The Palaeontological Association.

Martill D.M. (1993) - Soupy substrates: a medium for the exceptional preservation of ichthyosaurs of the Posidonia Shale (Lower Jurassic) of Germany. *Kaupia*, 2: 77–97.

Martini F.H. (1998) - The ecology of hagfishes. In: Jorgensen J.M., Lomholt, J.P., Weber, R.E. & Malte, H. (Eds) - Biology of Hagfishes: 57-77. Springer, Dordrecht.

Martire L. (1996) - Stratigraphy, facies and synsedimentary tectonics in the Jurassic Rosso Ammonitico Veronese (Altopiano di Asiago, NE Italy). *Facies*, 35: 209–236.

Martire L. & Clari P. (1994) - Evaluation of sedimentation rates in Jurassic-Cretaceous pelagic facies of the Trento Plateau: relevance of discontinuities and compaction. *Giornale di Geologia*, 56: 193–209.

Martire L., Clari P.A., Lozar F.& Pavia G. (2006) - The Rosso

Ammonitico Veronese (Middle–Upper Jurassic of the Trento Plateau): a proposal of lithostratigraphic ordering and formalization. *Rivista Italiana di Paleontologia e Stratigrafia*, 112: 227–250.

Massari F. (1981) - Cryptalgal fabrics in the Rosso Ammonitico sequences in the Venetian Alps. In: Farinacci A. & S. Elmi S. (Eds) - Rosso Ammonitico Symposium Proceedings: 435-469. Edizioni Tecnoscienza, Roma.

Massari F. & Westphal H. (2011) - Microbialites in the Middle–Upper Jurassic Ammonitico Rosso of the Southern Alps (Italy). In: Tewari V. & Seckbach J. (Eds) - Stromatolites: Interaction of Microbes with Sediments. Cellular Origin. Life in Extreme Habitats and Astrobiology, 18: 223–250.

Maxwell E.E. (2010) - Generic reassignment of an ichthyosaur from the Queen Elizabeth Islands, Northwest Territories, Canada. *Journal of Vertebrate Paleontology*, 30: 403–415.

Maxwell E.E., Cooper S.L., Mujal E., Miedema F., Serafini G. & Schweigert G. (2022) - Evaluating the existence of vertebrate deadfall communities from the Early Jurassic Posidonienschiefer Formation. *Geosciences*, 12(4): 158.

Mcneil B., Lowry D., Larson S. & Griffing D. (2016) - Feeding behavior of subadult sixgill sharks (*Hexanchus griseus*) at a bait station. *PLoS ONE*, 11: e0156730.

Merella M., Collareta A., Casati S., Di Cencio A. & Bianucci G. (2021) - An Unexpected Deadly Meeting: Deep-Water (Hexanchid) Shark Bite Marks on a Sirenian Skeleton from Pliocene Shoreface Deposits of Tuscany (Italy). *Neues Jahrbuch für Geologie und Paläontologie Abhandlungen*, 301: 295–305.

Merella M., Collareta A., Casati S., Di Cencio A. & Bianucci G. (2022) - Erratum: Merella, M, Collareta, A., Casati, S., Di Cencio, A., Bianucci, G. An Unexpected Deadly Meeting: Deep-Water (Hexanchid) Shark Bite Marks on a Sirenian Skeleton from Pliocene Shoreface Deposits of Tuscany (Italy). *Neues Jahrbuch für Geologie und Paläontologie Abhandlungen*. 2021, 301, 295–305. *Neues Jahrbuch für Geologie und Paläontologie Abhandlungen*, 303: 1–3.

Mironenko A.A. & Gulyaev D. (2018) - Middle Jurassic ammonoid jaws (anaptychi and rhynchaptychi) from Dagestan, North Caucasus, Russia. *Palaeogeography, Palaeoclimatology, Palaeoecology*, 489: 117–128.

Mironenko A.A., Jagt, J.W.M. & Jagt-Yazykova E.A. (2022) - An unusual conchorhynch from the upper Maastrichtian of the southeast Netherlands and the distinction between nautiloid and ammonoid conchorhynchs (Mollusca, Cephalopoda). *Cretaceous Research*, 130: 105037.

Moon B.C. & Kirton A.M. (2016) - Ichthyosaurs of the British Middle and Upper Jurassic. Part 1, *Ophthalmosaurus*. *Monographs of the Palaeontographical Society, London*, 170: 1–84.

Moon B.C. & Kirton A.M. (2018) - Ichthyosaurs of the British Middle and Upper Jurassic. Part 2, *Brachypterygius, Nannopterygius, Macropterygius* and Taxa invalida. *Monographs of the Palaeontographical Society, London*, 172: 85–177.

Nakano H., Hibino T., Oji T., Yuko H. & Amemiya S. (2003) - Larval stages of a living sea lily (stalked crinoid echinoderm). *Nature*, 421: 158–160.

Nixon M. (1988) - The buccal mass of fossil and recent cephalopods. In: Clarke M.R. & Treuman E.R. (Eds) - The Mollusca, Vol.12, Paleontology and Neontology of Cephalopods: 103-120. Academic Press, London.

Paparella I., Maxwell E., Cipriani A., Roncacè S. & Caldwell M.W. (2017) - The first ophthalmosaurid ichthyosaur

from the Upper Jurassic of the Umbrian–Marchean Apennines (Marche, Central Italy). *Geological Magazine*, 154: 837–858.

Parent H., Westermann G.E.G. & Chamberlain J.A. Jr. (2014) - Ammonite aptychi: Functions and role in propulsion. *Geobios*, 47: 45–55.

Pavia G., Benetti A. & Minetti C. (1987) - Il Rosso Ammonitico dei Monti Lessini Veronesi, Italia NE. Faune ad ammoniti e discontinuità stratigrafiche nel Kimmeridgiano Inferiore. *Bollettino della Società Paleontologica Italiana*, 26: 63–92.

Préat A., Morano S., Loreau J.P., Durlet C. & Mamet B. (2006) - Petrography and biosedimentology of the Rosso Ammonitico Veronese (middle-upper Jurassic, north-eastern Italy). *Facies*, 52: 265–278.

Préat A., Mamet B., Di Stefano P., Martire L. & Kolo K. (2011) - Microbially-induced Fe and Mn oxides in condensed pelagic sediments (Middle-Upper Jurassic, Western Sicily). *Sedimentary Geology*, 237(3-4): 179–188.

Perretti, C. T., Zerofski, P. J., & Sedarat, M. (2016) - The spawning dynamics of California market squid (*Doryteuthis opalescens*) as revealed by laboratory observations. *Journal of Molluscan Studies*, 82(1): 37-42.

Reisdorf A.G., Bux R., Wyler D., Benecke M., Klug C., Maisch M.W., Fornaro P. & Wetzel A. (2012) - Float, explode or sink: postmortem fate of lung-breathing marine vertebrates. *Palaeobiodiversity and Palaeoenvironments*, 92: 67–81.

Rees J. & Underwood C.J. (2008) - Hybodont sharks of the English Bathonian and Callovian (Middle Jurassic). *Palaeontology*, 51(1): 117–147.

Riegraf W. & Moosleitner G. (2010) - Barremian rhyncholites (Lower Cretaceous Ammonoidea: calcified upper jaws) from the Serre de Bleyton (Département Drôme, SE France). *Annalen des Naturhistorischen Museums in Wien. Serie A für Mineralogie und Petrographie, Geologie und Paläontologie, Anthropologie und Prähistorie*, 112: 627–658.

Robinson K.P., MacDougall D.A.I., Bamford C.C.G., Brown W.J., Dolan C.J., Hall R., Haskins G.N., Russell G., Sidiropoulos T., Sim T.M.C., Spinou E., Stroud E., Williams G. & Culloch R.M. (2023) - Ecological habitat partitioning and feeding specialisations of coastal minke whales (*Balaenoptera acutorostrata*) using a recently designated MPA in northeast Scotland. *PloS one*, 18(7): e0246617.

Rodríguez-Cabello C., González-Pola C., Rodríguez A. & Sánchez F. (2018) - Insights about depth distribution, occurrence and swimming behavior of *Hexanchus griseus* in the Cantabrian Sea (NE Atlantic). *Regional Studies in Marine Science*, 23: 60–72.

Roghi G. & Romano R. (2009) - Le Formazioni Geologiche del Veronese nella nuova Cartografia Geologica Nazionale. *La Lessinia, Ieri, Oggi e Domani. Quaderno n.* 32: 79-88.

Sarti C. (1993) - Il Kimmeridgiano delle Prealpi Veneto-Trentine: Fauna e Biostratigrafia. *Memorie del Museo Civico di Storia Naturale di Verona (serie* 2), 5: 1–154.

Sasaki T., Shigeno S. & Tanabe K. (2010) - Anatomy of living *Nautilus*: Reevaluation of primitiveness and comparison with Coleoidea. In: Tanabe K., Shigeta Y., Sasaki T. & Hirano H. (Eds) - Cephalopods - Present and Past: 35-66. Tokai University Press, Tokyo.

Sato, K. & Jenkins R.G. (2020) - Mobile home for pholadoid boring bivalves: first example from a Late Cretaceous sea turtle in Hokkaido, Japan. *Palaios*, 35: 228–236.

Schäfer W. (1972) - Ecology and Palaeoecology of Marine Environments. I. Oertel (trans.), G.Y. Craig (Ed.). Oliver &

Boyd, Edinburgh, 568 pp.

Schmeisser Mckean, R.L. & Gillette D.D. (2015) - Taphonomy of large marine vertebrates in the Upper Cretaceous (Cenomanian-Turonian) tropic shale of southern Utah. *Cretaceous Research*, 56: 278–292.

Schultz E.A., Cook M., Nero R.W., Caillouet R.J., Reneker J.L., Barbour J.E., Wang Z. & Stacy B.A. (2022) - Point of no return: determining depth at which sea turtle carcasses experience constant submergence. *Chelonian Conservation and Biology*, 21(1): 88–97.

Schwimmer D.R., Stewart, J.D. & Williams G.D. (1997) - Scavenging by sharks of the genus *Squalicorax* in the Late Cretaceous of North America. *Palaios*, 12(1): 71–83.

Séon N., Amiot R., Martin J.E., Young M.T., Middleton H., Fourel F., Picot L., Valentin X. & Lécuyer C. (2020) - Thermophysiologies of Jurassic marine crocodylomorphs inferred from the oxygen isotope composition of their tooth apatite. *Philosophical Transactions of the Royal Society B*, 375(1793): 20190139.

Serafini G., Amalfitano J., Cobianchi M., Fornaciari B., Maxwell E.E., Papazzoni C.A., Roghi G. & Giusberti L. (2020) - Evidence of opportunistic feeding between ichthyosaurs and the oldest occurrence of the hexanchid shark *Notidanodon* from the Upper Jurassic of Northern Italy. *Rivista Italiana di Paleontologia e Stratigrafia*, 126(3): 629–655.

Serafini G., Gordon C.M., Foffa D., Cobianchi M. & Giusberti L. (2022) - Tough to digest: first record of Teleosauroidea (Thalattosuchia) in a regurgitalite from the Upper Jurassic of north-eastern Italy. *Papers in Palaeontology*, 8: 1–22.

Serafini G., Maxwell E.E., Cobianchi M., Borghi L., Papazzoni C.A., Roghi G. & Giusberti L. (2023a) - Dead, discovered, copied and forgotten: history and description of the first discovered ichthyosaur from the Upper Jurassic of Italy. *Italian Journal of Geosciences*, 142(1): 131–148.

Serafini G., Foffa D., Young M.T., Friso G., Cobianchi M., Giusberti L. (2023b) - Reappraisal of the thalattosuchian crocodylomorph record from the Middle-Upper Jurassic Rosso Ammonitico Veronese of northeastern Italy: age calibration, new specimens and taphonomic biases. *Plos One*, 18(10): e0293614.

Serafini G., Amalfitano J., Danise S., Maxwell E.E., Rondelli R. & Papazzoni C.A. (2023c) - Not entirely ichthyosaur: a mysterious lamniform and ichthyopterygian-fall association from the abyssal Upper Cretaceous of the northern Apennines (Italy). *Palaios*, 38 (8): 331–344.

Sirna G., Dalla Vecchia F.M., Muscio G. & Piccoli G. (1994) - Catalogue of Paleozoic and Mesozoic vertebrates and vertebrate localities of the Tre Venezie area (North Eastern Italy). *Memorie di Scienze Geologiche*, 46: 255–281.

Sissons R.L., Caldwell M.W., Evenchick C.A., Brinkman D. & Vavrek M. (2015) - An Upper Jurassic ichthyosaur (Ichthyosauria: Ophthalmosauridae) from the Bowser Basin, British Columbia. *Canadian Journal of Earth Sciences*, 52: 1–7.

Smith C.R. & Baco A.R. (2003) - Ecology of whale falls at the deep-sea floor. *Oceanography and Marine Biology: an Annual Review*, 41: 311–354.

Smith C.R., Glover A.G., Treude T., Higgs N.D. & Amon D.J. (2015) - Whale-fall ecosystems: recent insights into ecology, paleoecology, and evolution. *Annual Review of Marine Science*, 7: 571–596.

Stinnesbeck W., Frey E., Rivas L., Pardo-Pérez J., Leppe M., Salazar C. & Zambrano Lobos P. (2014) - A Lower Cretaceous ichthyosaur graveyard in deep marine slope channel deposits at Torres del Paine National Park, Southern Chile. *Geological Society of America Bulletin*, 126: 1317–1339.

Tanabe K., Kruta I. & Landman N.H. (2015) - Ammonoid buccal mass and jaw apparatus. In: Klug C., Korn D., De Baets K., Kruta I. & Mapes R.H. (Eds) - Ammonoid Paleobiology: From Anatomy to Ecology. Topics in Geobiology, 43: 439–494. Springer, Dordrecht.

Treude T., Smith C.R., Wenzhöfer F., Carney E., Bernardino A.F., Hannides A.K., Krüger M. & Boetius A. (2009) - Biogeochemistry of a deep-sea whale fall: sulfate reduction, sulfide efflux and methanogenesis. *Marine Ecology Progress Series*, 382: 1–21.

Trueman C.N. & Martill D.M. (2002) - The long-term survival of bone: the role of bioerosion. *Archaeometry*, 44: 371–438.

Wahl W.R. (2009) - Taphonomy of a nose dive: bone and tooth displacement and mineral accretion in an ichthyosaur skull. *Paludicola*, 7: 107–116.

Winterer E.L. (1998) - Paleobathymetry of Mediterranean Tethyan Jurassic pelagic sediments. *Memorie della Società Geologica Italiana*, 53: 97–131.

Winterer E.L. & Bosellini A. (1981) - Subsidence and Sedimentation on a Jurassic Passive Continental Margin, Southern Alps, Italy. *American Association of Petroleum Geologists Bulletin*, 65(3): 394–421.

Wisshak M., Knaust D. & Bertling M. (2019) - Bioerosion ichnotaxa: review and annotated list. *Facies*, 65: 24.

Young M.T., Bell M.A., Andrade M.B. & Brusatte S.L. (2011) - Body size estimation and evolution in metriorhynchid crocodylomorphs: implications for species diversification and niche partitioning. *Zoological Journal of the Linnean Society*, 163: 1199–1216.

Young M.T., Brusatte S.L., Andrade M.B., Desojo J.B., Beatty B.L., Steel L., Fernandez M.S., Sakamoto M., Ruiz-Omeñaca J.I. & Schoch R.R. (2012) - The cranial osteology and feeding ecology of the metriorhynchid crocodylomorph genera *Dakosaurus* and *Plesiosuchus* from the Late Jurassic of Europe. *PLoS One*, 7: e44985.

Zempolich W.G. (1993) - The Drowning Succession in Jurassic Carbonates of the Venetian Alps, Italy: A Record of Supercontinent Breakup, Gradual Eustatic Rise, and Eutrophication of Shallow-Water Environments. In: Loucks R.G. & Sarg J.F. (Eds) - Carbonate Sequence stratigraphy-Recent Developments and Applications. *AAPG Memoir*, 57: 63–105.

Zverkov N.G. & Efimov V.M. (2019) - Revision of *Undorosaurus*, a mysterious Late Jurassic ichthyosaur of the Boreal Realm. *Journal of Systematic Palaeontology*, 17: 1183e1213.

Zverkov N.G. & Jacobs M.L. (2021) - Revision of *Nannopterygius* (Ichthyosauria: Ophthalmosauridae): reappraisal of the 'inaccessible' holotype resolves a taxonomic tangle and reveals an obscure ophthalmosaurid lineage with a wide distribution. *Zoological Journal of the Linnean Society*, 191(1): 228-275.